Accepted Manuscript

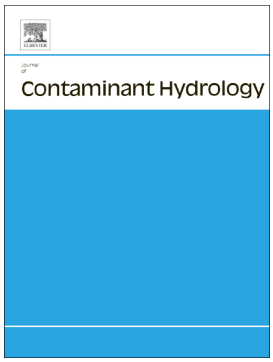

Realistic expectations for the treatment of FMGP residuals by chemical oxidants

Saeid Shafieiyoun, Neil R. Thomson, Andrew P. Brey, Chris M. Gasinski, W. Pence, Mike Marley

PII: S0169-7722(17)30251-6
DOI: doi:10.1016/j.jconhyd.2018.08.007
Reference: CONHYD 3417

To appear in: *Journal of Contaminant Hydrology*

Received date: 25 August 2017
Revised date: 29 June 2018
Accepted date: 29 August 2018

Please cite this article as: Saeid Shafieiyoun, Neil R. Thomson, Andrew P. Brey, Chris M. Gasinski, W. Pence, Mike Marley , Realistic expectations for the treatment of FMGP residuals by chemical oxidants. Conhyd (2018), doi:10.1016/j.jconhyd.2018.08.007

Submitted to Journal of Contaminant Hydrology

Realistic Expectations for the Treatment of FMGP Residuals by Chemical Oxidants

Saeid Shafieiyoun[1,*], Neil R. Thomson[1], Andrew P. Brey[2], Chris M. Gasinski[3], W. Pence[4], Mike Marley[5]

[1]Department of Civil and Environmental Engineering
University of Waterloo, 200 University Avenue West,
Waterloo, ON N2L 3G1

[2]Geosyntec Consultants, 5
13101 Telecom Drive, Suite 120,
Temple Terrace, FL 33637

[3]TECO Peoples Gas
702 Franklin Street North,
Tampa, FL 33602,

[4]Baker & Hostetler LLP
200 South Orange Avenue, Suite 2300,
Orlando, FL 32801-3432

[5]XDD Environmental LLC
22 Marin Way, Unit #3,
Stratham, NH 03885

*corresponding author; e-mail:s5shafie@uwaterloo.ca

Abstract

Methods to remediate soil and groundwater contamination at former manufactured gas plant (FMGP) sites are scarce. The objective of this study was to investigate the ability of two chemical oxidants (persulfate and permanganate) to degrade FMGP residuals in a dynamic system representative of *in situ* conditions. A series of physical model trials supported by aqueous and slurry batch experiments using impacted sediments collected from a FMGP site were conducted. To explore treatment expectations a screening model constrained by the experimental data was employed. The results from the aqueous experiments showed that dissolved components (except for benzene) were readily degraded by persulfate or permanganate. In the well-mixed slurry systems, when contact with the oxidant was achieved, 95%, 45% and 30% of the initial mass quantified was degraded by permanganate, unactivated persulfate, and alkaline activated persulfate, respectively. In stark contrast, the total mass removed in the physical model trials was negligible for both permanganate and persulfate irrespective of the bleb or lense architecture used. Hence the net benefit of flushing 6 pore volumes of permanganate or persulfate at a concentration of 30 g/L under the physical model operating conditions was minimal. To achieve a substantial degradation of mass within the treatment system (> 40 %), results from the screening model indicated that the hydraulic resident time would need to be > 10 days and the average lumped mass transfer coefficient increased by two orders-of-magnitude. Results from long-term (5 years) simulations showed that the dissolved concentrations of organic compounds are reduced temporality as a result of the presence of permanganate but then rebound to a profile that is essentially coincident with a no-treatment scenario following exposure to permanganate. Neither a lower velocity nor higher permanganate dosing affected the long-term behavior of the dissolved phase concentrations; however, increasing the mass transfer rate coefficient had an impact. The findings from this investigation indicate that the efficiency of permanganate or persulfate to treat for FMGP residuals is mass transfer limited.

Keywords: coal tar, MGP, persulfate, permanganate, mass transfer, treatment end-points, long-term expectations

1.0 Introduction

Prior to 1950, thousands of manufacturing plants produced a combustible gas from coke, coal or oil that was used in urban environments for lighting, heating, and cooking (Hatheway, 2012). Due to poor process operations and residual management practices, there currently exists serious soil and groundwater contamination problems at many of these former manufactured gas plant (FMGP) sites (Cassidy et al., 2015; Wang et al., 2015; Hauswirth et al., 2012, USEPA, 1999). FMGP residuals are usually found in the subsurface as non-aqueous phase liquids (NAPLs) that are typically denser and more viscous relative to water, and are composed of hundreds to thousands of organic compounds (Mueller et al., 1989). Based on observations from various site characterization efforts, the *in situ* architecture of these coal tar NAPLs range from sheens, stains, tar blebs and tar coatings to saturated lenses or pools. Despite vast advancements in analytical methods, it is currently only possible to quantify a portion of the organic compounds present in FMGP coal tars, and even the analysis of this identified portion is extremely complicated (Birak & Miller, 2009). Moreover, the composition of FMGP tars varies between sites due to differences in source material and processing operations (Birak & Miller, 2009; Luthy et al., 1994). When FMGP tars are initially exposed to groundwater, the more soluble compounds will gradually be depleted over time (a phenomenon called aging or weathering) and the higher molecular weight compounds, which are generally the less soluble compounds, will remain in the NAPL. The presence of these FMGP tars in subsurface environments may pose a long-term threat to groundwater quality and potentially human health if left untreated or if potential exposure pathways are not appropriately addressed.

Remediation initiatives at many FMGP sites have been limited to isolation or removal of the source materials (USEPA, 2013; Birak & Miller, 2009; Luthy et al., 1994). Over the last 15 years, *in situ* chemical oxidation (ISCO) has been growing steadily as a remediation technology used to treat a range of environmentally relevant contaminants (Siegrist et al., 2011). Although different types of chemical oxidants have been employed, persulfate and permanganate are the two most frequently used as they are typically more persistent in subsurface systems (Petri et al., 2011a,b; USEPA, 2006). Since chemical oxidation has been shown to successfully degrade a number of the dissolved organic compounds typically present at FMGP sites (polyaromatic hydrocarbons (PAHs); benzene, toluene, ethylbenzene, and xylenes (BTEX)) (Sra et al,

2013; Forsey et al, 2010), it is speculated that it could be a beneficial technology to treat FMGP tars *in situ*.

Published studies dealing with the chemical oxidation of FMGP residuals have been diverse in scope with varied and often conflicting results. Table 1 provides a comprehensive summary of published bench-scale studies which have used either persulfate or permanganate to degrade FMGP residuals in batch (i.e., well-mixed slurry) or column systems.

Some of the investigations detailed in Table 1 have used impacted aquifer or river sediments collected from FMGP sites, while others have used soils "spiked" with a MGP NAPL (Peng et al., 2016; Usman et al., 2012; Brown et al., 2003). Although spiked-soil studies provide valuable insight into the chemical reactivity of different oxidants to attack MGP residuals, the use of impacted materials collected from FMGP sites better represents the *in situ* chemical composition. Employing a series of batch experiments, Usman et al. (2012) observed that magnetite-activated persulfate was able to degrade 70 to 80% of the total PAHs (PAH_T) in spiked sand, but when a FMGP soil was used no PAH mass was removed. In contrast, Cassidy et al. (2015) reported mass removal of 55 to 65% using alkaline-activated persulfate (~37 g/L) in a batch system for soil material with an initial BTEX concentration of 0.58 g/kg, and a PAH_T concentration of 3.06 g/kg (sum of 18 compounds). Nadim et al. (2005) observed between 75 to 100% PAH_T removal (7 compounds) using iron-activated persulfate (5 g/L) for a less impacted soil (0.01 g/kg PAH_T). Only a few studies have directly compared the effectiveness of different chemical oxidants to degrade organic mixtures (Lemaire et al., 2013; Ferrarese et al., 2008; Rivas 2006; Gates-Anderson et al., 2001). For example, Ferrarese et al. (2008) identified that a 158 g/L permanganate solution and a 120 g/L persulfate solution were able to degrade 96 and 88% of the PAH_T present in impacted soil with an initial PAH_T concentration of 2.8 g/kg, respectively.

Batch systems normally provide the most ideal environment to maximize treatment due to high oxidant dosing (mass of oxidant/mass of contaminant), maximum contact between the oxidant and the NAPL (well-mixed), and long reaction or residence times. In contrast, column systems are often considered more representative of a dynamic subsurface situation where preferential pathways exist, there is less direct oxidant contact with the NAPL, and the residence time is controlled by the flow system. For example, despite a PAH_T removal of 47% (14 compounds) in a series of batch experiments, Richardson et al. (2011) observed no reduction in PAH mass from column

experiments using a heat-activated persulfate system in spite of a relatively low PAH_T concentration of ~0.3 g/kg. In comparison, Hauswirth and Miller (2014) performed column experiments using FMGP impacted soils (initial PAH_T concentration of 1.99 g/kg of tar; 25 compounds) and reported a 53% removal of PAH_T after injecting 52 pore volumes (PVs) of a 50 g/L alkaline-activated persulfate solution. Since a typical field injection event is < 1 PV (Huling et al., 2017; Crimi et al., 2011), this high number of PVs is impractical at most field sites and hence the results from this column experiment should be viewed as highly optimistic.

In addition to the ability of chemical oxidants to degrade multi-component NAPLs such as FMGP residuals, aquifer material and NAPL architecture, in part, dictate contaminant availability and consequently treatment effectiveness (Zhang et al. 2007). The NAPL surface area to volume ratio is much less for a lense or pool architecture compared to bleb architecture, and hence the relative surface or contact area is lower (Powers et al., 1994a). Moreover, the aqueous hydraulic conductivity is reduced within regions with a lense architecture, and thus the ability to flush remedial fluids into these areas is limited (Zhang et al., 2008). This will restrict the efficiency of a chemical oxidation system, and in such conditions multiple injection episodes to effectively degrade the NAPL are required (Petri et al., 2011a).

Due to complex entrapment and multicomponent aspects of FMGP residuals it is generally not possible to remove all of the NAPL mass during treatment with a chemical oxidant (Soga et al., 2004). For example, Thomson et al. (2008) monitored the short-term (months) and long-term (years) behaviour of a plume originated from a multi-component NAPL source zone after treatment with permanganate. They concluded that, while the short-term organic compound concentrations were reduced significantly, there was rebound of all of the monitored compounds after four years post-treatment. Hence, predicting the long-term behaviour of dissolved phase concentrations following chemical oxidation treatment is necessary for the evaluation of post-treatment expectations and risk assessment. The few studies that have investigated the long-term behavior of dissolved phase concentrations from FMGP residuals have indicated that dissolution kinetics depends on NAPL composition, and the time scale for complete removal can vary between weeks to more than thousands of years for different NAPL architectures (Eberhardt & Grathwohl, 2002).

Based on the current literature (Table 1), it is unclear what the dissolved phase concentration behaviour is following treatment of FMGP tars with different NAPL

architectures by various chemical oxidants. The objective of this study was to investigate the performance of two chemical oxidants (sodium persulfate ($Na_2S_2O_8$) and potassium permanganate ($KMnO_4$)) to degrade FMGP residuals in a continuous flow system representative of *in situ* conditions. Specifically, the focus was on the ability of each oxidant to remove FMGP residual mass, and the impact on the dissolved phase concentrations following treatment. Supported by aqueous and slurry batch experiments, a series of physical model trials were conducted using impacted sediments collected from a FMGP site. The aqueous experiments focused on the ability of permanganate and three persulfate systems to degrade impacted groundwater collected from a FMGP site at both low and high initial oxidant concentrations. In contrast, the slurry experiments were used to quantify the potential of permanganate and three persulfate systems to remove mass from aquifer sediments containing FMGP residuals. Each physical model was subjected to three oxidant flushing episodes (6 PVs in total) and the effluent was sampled between each episode. At the termination of each trial, sediment samples were collected from the physical model and analyzed for a suite of organic compounds to determine mass removed. A simple single-cell screening model constrained by the experimental results was used to investigate treatment expectations, and the potential long-term behaviour of dissolved phase concentrations as a result of treatment using these chemical oxidants.

2.0 Materials and Methods

2.1 Aquifer materials and NAPL

Impacted groundwater and FMGP residuals used in this study were obtained from the former West Florida Natural Gas Company Site located in Ocala, Florida. From the late 1890s until about 1953, water gas or carbureted water gas was manufactured at this location by the “Lowe” carbonization process or destructive distillation of bituminous coal and coke. According to Brown's Directory of North American Gas Companies (1964), gas production was ~48 x 10^3 m^3/yr in 1900 and steadily increased to 900 x 10^3 m^3/yr by 1950. In 1952, manufacturing stopped at the plant and the facility converted to the sale of butane-propane-air. Residues from the MGP process, including tars and oily wastewaters, were deposited in the area of the former gas plant facilities during

operations. There was an historic coal tar pit or area where residual tars were stored prior to sale for off-site use as roofing materials.

Groundwater samples were collected in 1000 mL amber glass containers from two monitoring wells screened from 19.8 to 21.3 and 36.0 to 39.6 m below ground surface (bgs) utilizing a low flow (< 0.2 L/min) purge sampling technique. The samples were placed in coolers maintained at ~4 °C and transported to the University of Waterloo where they were stored in a walk-in refrigerator at 4 °C.

During extensive drilling activities at the site, both impacted and non-impacted aquifer materials were collected from a weathered limestone unit using rotosonic drilling methods. Cores were recovered in 1.5 m runs using a 10.2 cm diameter core barrel with a button-carbide drill bit. Core materials assigned as "impacted weathered limestone unit material" and "non-impacted weathered limestone unit material" collected from inside the delineated source zone were used in this investigation. The weathered limestone unit is part of an erosional surface of the Miocene Age, and its composition includes clayey limestone, sandy limestone and limey clay. Impacted aquifer material was immediately transferred into 500 mL glass jars, sealed with a self-sealing lid held in place with a metal screw-top ring, and stored on-site in a freezer at -20 °C (see Figure SM-1(a) in the Supplementary Material (SM) section). Non-impacted aquifer material was stored in polyethylene bags (Figure SM-1(b)). Samples of impacted aquifer material were collected from two boreholes, and are representative of depths ranging from 10 to 30 m bgs, while non-impacted aquifer materials were collected from five boreholes and are representative of depths ranging from 15 to 20 m bgs. Sufficient core materials were express shipped to the University of Waterloo on ice. Samples of the impacted aquifer materials were stored at -40 °C, while samples of the non-impacted aquifer materials were stored at 4 °C. The inventory of impacted aquifer materials received was visually inspected and separated into two categories based on NAPL presence. Lower impacted aquifer materials were reserved for the slurry treatability and the "bleb" architecture physical model experiments, while the higher impacted aquifer materials were reserved for the "saturated lense" architecture physical model experiments (Figure SM-2).

A NAPL sample (density of 1.04 g/cm^3) collected from a well screened from 24 to 27 m bgs within the weathered limestone was submitted to Alpha Analytical Laboratories Westborough, MA for analyses of BTEX, total petroleum hydrocarbons (TPH), and PAHs. A summary of these results are listed in Table SM-1 and indicate that ~34% of the NAPL mass was quantified (66% of the NAPL mass was unidentified). Consistent

with the composition of other FMGP NAPLs (e.g., Brown et al. 2006) the most abundant compounds in the quantified portion of the NAPL are naphthalene (24.6 %), 2-methylnaphthalene (13.7 %), 1-methylnaphthalene (7.5 %), and acenaphthene (3.9 %). The benzene concentration represented ~0.8 % of the quantified portion of the NAPL. For illustrative purposes in this paper, we chose to report on the behaviour of naphthalene, acenaphthene and benzene; naphthalene and acenaphthene as a result of their higher NAPL concentration, and benzene since it is typically a risk driver.

2.2 Natural Oxidant Interaction

Naturally occurring reductants and catalysts can be reactive and thus influence oxidant persistence. Typically, the role of the dissolved groundwater species is overshadowed by the aquifer solids. Inorganic species containing iron (Fe), manganese (Mn), sulfur (S), and the natural organic matter (NOM) associated with the aquifer solids are of concern. The possibility of multiple inorganic species, as well as a range of NOM, creates an extremely heterogeneous environment in which reactions may occur. The result of the interaction between an oxidant and aquifer material leads to either an increase in the consumption of the oxidant by the aquifer solids, or an enhancement in the oxidant decomposition rate. When an oxidant is consumed by the aquifer solids, the reactive species associated with the aquifer solids are finite, and hence there exists a finite consumption or natural oxidant demand (NOD). Once the maximum NOD is satisfied, there is minimal additional oxidant aquifer material interaction and, thus, any additional oxidant delivered is available to interact with the contaminant. Conversely, an enhancement in the oxidant decomposition rate implies that there is infinite interaction capacity available. To capture these behavioral differences and the associated underlying processes for all oxidant behavior the term natural oxidant interaction (NOI) is used rather than NOD.

NOI tests were used to estimate the potential *in situ* interaction of persulfate and permanganate with non-impacted aquifer materials from three (3) representative locations. For these NOI tests the oxidant mass to solids ratio ranged from 5 to 40 g/kg (nominal). NOI tests were conducted for three persulfate systems: (1) unactivated persulfate, (2) chelated ferrous iron activated persulfate, and (3) alkaline activated persulfate. Details of the experimental procedures employed are provided in the SM section.

2.3 Aqueous Treatability Experiments

Since the chemical oxidation of organic compounds occurs in the aqueous phase, experiments were conducted using impacted groundwater exposed to permanganate or persulfate (unactivated, ferrous iron activated (300 mg/L Fe(II) + 0.5 mol citric acid/mol Fe(II)), or alkaline activated) to determine aqueous degradation characteristics. A suite of five (5) tests was executed in well-mixed 20 mL batch reactors. Each test was performed in triplicate at a low (5 g/L) and a high (30 g/L) oxidant concentration in conjunction with experimental controls (i.e., impacted groundwater and 0.2 mL of 10% NaN_3; and impacted groundwater adjusted with NaOH to an initial pH of 11). Impacted groundwater was added to each reactor followed by the activator solution (if required) and then the oxidant. Initial reactor solution volumes were adjusted with Milli-Q water, as required, to ensure the same dilution of groundwater across all tests. Reactors were shaken gently by-hand at least daily and left in the dark at an ambient temperature of ~20 °C. Aliquots of the solution were taken after a reaction period of 1, 4, 8, 15 and 30 days, and analyzed for the concentrations of a suite of 28 organic compounds (Table SM-4) and the oxidant. The solution pH was also determined.

2.4 Slurry Treatability Experiments

A series of experiments were performed to capture the ability of the various oxidant systems (permanganate and persulfate) to degrade impacted aquifer sediments. The impacted weathered limestone unit material selected for these slurry treatability experiments were opened, emptied onto a sterilized tray, and homogenized. Minimal Milli-Q water was added as required to improve mixing. Large size particles that were not suitable for the reactor design were removed by-hand during mixing. Random samples from the homogenized mixture were used without additional alteration. Prior to filling the reactors, five (5) sub-samples from the homogenized mixture were collected and used to establish the initial bulk soil concentrations. A 75 g random sample of the impacted sediments was added to a 125 mL reactor, followed by a 30 g/L oxidant solution (permanganate, unactivated persulfate, and alkaline activated persulfate) to achieve an oxidant mass to solids ratio of 30 g/kg (nominal). All reactors were constructed in replicates (4), and constantly mixed on a shaker table in the dark at an ambient temperature of ~20 °C. Every 7 days for a 35-day period the oxidant concentration and pH were determined, and a random sediment sub-sample from each reactor was collected and analysed to determine bulk soil concentrations. If the results

from a sampling episode indicated that the oxidant concentration was depleted, additional oxidant mass was added to achieve a solution concentration of 30 g/L.

2.5 Physical Model Experiments

For the purpose of the evaluation conducted in this study, we assumed that NAPL architecture that is characterized as sheens, staining, tar blebs, and tar coatings have a similar architecture with respect to the ability of a reagent solution to interact with the NAPL. When these NAPL forms are present in a permeable setting, there is a good likelihood of contact between the reagent solution and the NAPL. However, when the NAPL is present as a NAPL-saturated lense, the ratio of NAPL surface area to volume is significantly smaller and reagent/NAPL contact becomes problematic. The series of small-scale physical model experiments performed were designed with the intention to capture the two NAPL architecture end-points: blebs and tar coatings, and saturated lenses.

The physical model was a 7.7 cm long flow-through chamber with a cross-sectional area of 8.37 cm^2 (3.1 x 2.7 cm) (Figure 1). The influent and effluent ends of the chamber were packed with a 0.8 cm long zone of glass beads (diameter 1.6 mm) and a #20 stainless steel mesh to act as a flow distributor. The remaining 6.1 cm length was wet packed with impacted aquifer sediments. The chamber was sufficiently filled that when the lid was fastened it compressed the chamber contents, ensuring a seal between the top of the chamber contents and the bottom of the lid to eliminate short-circuiting of injected fluids. For the "bleb" system, impacted materials were packed gradually in several 0.5 cm thick layers into the central portion of the physical model. For the "saturated lense" system, impacted samples were emptied directly into the bottom of the physical model to a depth of ~1.5 cm and the upper ~1.5 cm portion of the chamber was then packed with non-impacted material from the same borehole. During the filling process, five sub-samples were taken and used to establish the initial bulk soil concentrations. This system was then saturated with degassed Milli-Q water and allowed to equilibrate for 7 days.

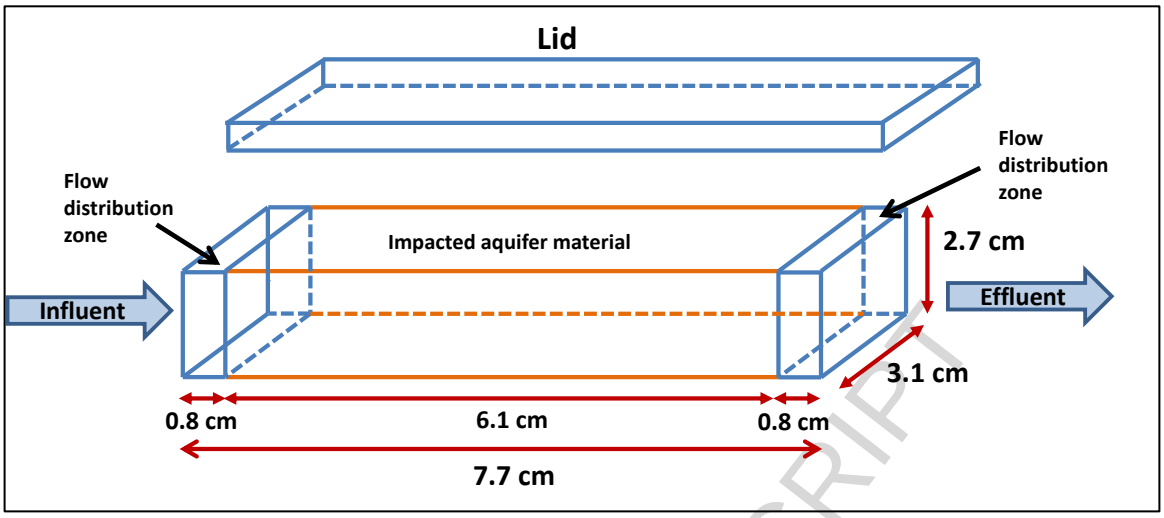

Figure 1. Schematic of physical model chamber with a length of 7.7 cm and cross-sectional area of 8.37 cm^2 (3.1 cm x 2.7 cm). The influent and effluent ends were packed with a 0.8 cm long zone of glass beads. The interior 6.1 cm long zone was packed with impacted aquifer materials.

Following the 7-day equilibration period, flow was initiated at a nominal rate of 0.017 mL/min (approximate linear velocity of 10 cm/day). A peristaltic pump was connected to the influent end and a constant hydraulic head control was established at the outlet end. An in-line sampling system allowed aqueous samples to be collected from the effluent as required. A tracer test using NaBr was performed on each model system to ensure hydraulic consistency and packing. Following the tracer test, three oxidant injection episodes were performed. Between each episode, degassed Milli-Q water was used to remove remnant oxidant from the system and facilitate the collection of aqueous effluent samples for analysis of organic compounds. Specifically, each physical model system was operated in the following sequence of steps:

(1) One PV of degassed Milli-Q water was injected to displace the pore water and allowed to equilibrate in the system for 7 days.

(2) Three to four PVs of 100 mg/L degassed NaBr solution were injected. During the tracer test, effluent samples were collected every 4 hours.
(3) At the end of the tracer test, an effluent sample was collected to establish a baseline effluent organic compound concentration signature.
(4) Two PVs of oxidant (permanganate or persulfate) at a concentration of 30 g/L were injected. During each oxidant injection episode, the effluent was sampled at least 4 times for electrical conductivity (EC), pH, and oxidant concentration.
(5) Three PVs of degassed Milli-Q water were injected. The system effluent was monitored for EC, pH and oxidant concentration during the initial 2 PVs to ensure remnant oxidant was removed from the system. During the third PV, an effluent sample was collected to determine the concentration of organic compounds in the effluent
(6) Steps (4) and (5) were then repeated twice more (3 oxidant injection episodes in total).
(7) When the experimental test was concluded, the chamber lid was removed and three sub-samples equally spaced along the length of the chamber were collected to establish post-treatment bulk soil concentrations. For the “saturated lense” system, the sub-samples were collected only from the lower ~1.5 cm portion of the chamber that contained impacted material.

The sampling protocol followed in Step (5) was adopted since the results from a series of preliminary experiments showed that when persulfate or permanganate was present in the effluent from the physical model the concentration of the organic compounds of interest were <MDL (for example, see Table SM-5). Additionally, our focus was on the rebound of the dissolved phase concentrations following treatment since this behavior is of interest to remediation practitioners and regulatory agencies (Thomson et al, 2008; McGuire at at, 2006).

Since the system PV and porosity was unknown at the start of each experiment, a nominal PV of 19.33 mL was used. This nominal PV was estimated from a porosity of 0.3 determined from a set of preliminary experiments, and the packed chamber volume of 64.45 mL (7.7 cm x 2.7 cm x 3.1 cm). The nominal hydraulic residence time was ~20 hrs. Four physical systems were constructed for the "bleb" architecture, and four systems for the "saturated lense" architecture. Permanganate (30 g/L) was used for two "bleb" systems (identified as PM-bleb-1 and PM-bleb-2), and two "saturated lense" systems (identified as PM-lense-1 and PM-lense-2). Persulfate (30 g/L) was used for the

remaining two "bleb" systems (identified as PS-bleb-1 and PS-bleb-2), and two "saturated lense" systems (identified as PS-lense-1 and PS-lense-2). Based on the results from the aqueous and slurry batch experiments, persulfate activator systems were not investigated. In addition, two systems were constructed as experimental controls and identified as CO-bleb and CO-lense. The experimental controls received only degassed Milli-Q water. The oxidant concentration (30 g/L) was selected to mimic a potential concentration for a site where density driven advection of the injected oxidant solution is of concern.

2.6 Reagents and Analytical Methods

Potassium permanganate ($KMnO_4$, EM Science), sodium persulfate ($Na_2S_2O_8$, Sigma-Aldrich Inc.), sodium hydroxide (NaOH, Fisher Scientific), ferrous sulfate ($FeSO_4 \cdot 7H_2O$, Sigma-Aldrich), metafluoro-toluene (C_7H_7F, Sigma-Aldrich), fluoro-biphenyl ($C_{12}H_9F$, Sigma-Aldrich), sodium bromide (NaBr, Sigma-Aldrich), citric acid ($C_6H_8O_7$, Sigma-Aldrich), and dichloromethane (DCM, EMD Millipore) were all reagent grade and used as received.

For analysis of the organic components in the aqueous phase, a 5 mL sample was mixed with 14 mL of water in a 20 mL vial. This was followed immediately by the addition of 1.0 mL of DCM (containing internal standards metafluoro-toluene (MFT) and fluoro-biphenyl (FBP) at 25 mg/L). The vial was quickly resealed and agitated on its side at 350 rpm on a platform shaker for 20 min. After shaking, the vial was inverted and the phases were allowed to separate for 30 min. Approximately 0.7 mL of the DCM was removed from the inverted vial with a gas tight glass syringe through the Teflon septum. The solvent was placed in a 2.0 mL Teflon sealed autosampler vial for injection into the gas chromatograph (GC). For the analysis of the organic components in the aquifer sediment, an ~8 g sub-sample was added directly to 10 mL of DCM and shaken for 18 hours. Samples were allowed to settle and 1 mL of the DCM was transferred to a 2.0 mL autosampler vial and crimp sealed with a Teflon cap. All aqueous and sediment samples were analyzed using a HP 5890 capillary GC, a HP7673A autosampler, and a flame ionization detector. Three (3) µL of DCM was injected in splitless mode (purge on 0.5 min, purge off 10 min) onto a 0.25 mm x 30 m length, DB5 capillary column with a stationary phase film thickness of 0.25 µm. The helium column flow rate was 2.0 mL/min with a make-up gas flow rate of 30 mL/min. The injection temperature was 275 ^{o}C, detector temperature was 325 ^{o}C and initial column oven temperature was 35 ^{o}C held for 0.5 min, then ramped up at 15 ^{o}C/min to a final temperature of 250 ^{o}C and held for 2 min.

A GC run time was 16 min. Data integration was completed with a SRI Model 302 Peak Simple chromatography data system. The method detection limit (MDL) for each quantified compound determined in the aqueous or sediment phase is presented in Table SM-4. Using these analytical methods we are able to track 28 compounds or ~27 % of the compounds in the NAPL mass (Table SM-1). The behaviour of the compounds that comprise the other ~70 % of the NAPL mass is unknown.

Permanganate concentration was determined by spectrophotometry (Thermo Scientific, GENESYS 10S UV-Vis) at 525 nm (MDL of 1.3 mg/L). The spectrophotometer was calibrated prior to each sampling episode with a calibration curve (1 to 100 mg/L) generated using standardized solutions. Persulfate analysis was performed following Liang et al. (2008). Bromide (Br^-) was analyzed using a Dionex ICS2000 Ion Chromatograph equipped with an ion eluent generator and conductivity detector. A 25-µL sample was injected using a Dionex AS-40 Autosampler onto a Dionex Ion Pac AS11-HC (4 × 250 mm) column. The mobile phase was 30 mM potassium hydroxide (KOH) at a flow rate of 1.0 mL/min. The chromatograph was obtained using Dionex Chromeleon software and the MDL was 0.5 mg/L. An Orion pH meter (model 290A) and EC meter (model A122) were used to measure pH and electrical conductivity.

2.7 Screening Model

To explore expectations for the treatment of FMGP residuals by chemical oxidants, a single-cell screening model was employed. In this model, a specified mass and composition of NAPL is assumed to be present within the sediment, and the aqueous phase is presumed completely mixed. The inlet oxidant concentration is prescribed and the effluent concentrations of the known soluble constituents are estimated from mass balance considerations. The objective of this *idealized* modeling effort was to provide insight into treatment expectations under different operating conditions then those employed in the physical model experiments and over longer time scales. It was not our intent to simulate *in situ* conditions, but rather to investigate what might be possible under ideal circumstances and hence yield the most optimistic predictor of field behavior. This screening model was deemed an appropriate tool to satisfy this requirement.

The mass balance of the individual soluble NAPL constituents is given by

$$\frac{dC_k}{dt} = -\frac{C_k}{t_r} - k_{ox,k} C_{ox} C_k + \lambda_k (C_k^{eff} - C_k) \quad (1)$$

with

$$\frac{dM_k}{dt} = -\lambda_k \theta (C_k^{eff} - C_k) V_s \quad (2)$$

$$C_k^{eff} = \frac{x_k \gamma_k S_k}{(f^S / f^L)_k} \quad (3)$$

$$\lambda_k = \beta_o D_k^w \left(v \rho_w / \mu_w\right)^{0.598} \left(\theta_n / \theta_{no}\right)^{0.667} \quad (4)$$

and

$$t_r = \frac{L_s}{v} = \frac{\theta L_s}{q} \quad (5)$$

where C_k is concentration of the k^{th} constituent, t_r is the system hydraulic residence time, $k_{ox,k}$ is the second-order reaction rate coefficient with respect to the oxidant for the k^{th} constituent, C_{ox} is the oxidant concentration, λ_k is the lumped mass transfer rate coefficient for the k^{th} constituent which is estimated from Eq (4) adopted from Powers et al. (1994b), C_k^{eff} is the effective saturation of the k^{th} constituent, M_k is the NAPL mass associated with the k^{th} constituent, θ is the system porosity, V_s is the volume of the system, x_k is the mole fraction of the k^{th} constituent, γ_k is the activity coefficient of the k^{th} constituent, S_k is the solubility of the k^{th} constituent, f^S and f^L are the fugacity of the solid and liquid of the k^{th} constituent, β_o is a coefficient determined by lumping soil properties in the mass transfer rate coefficient correlation of Powers et al. (1994b), D_k^w is the free solution diffusion coefficient for the k^{th} constituent estimated from Wilke and Chang (1955), μ_w is the aqueous viscosity, ρ_w is the aqueous density, θ_n is the volumetric fraction of NAPL ($S_n\theta$), θ_{no} is initial volumetric fraction of NAPL in the system, L_s is the system length, v is velocity, and q is Darcy flux. Lee et al. (1992) investigated the aqueous equilibrium concentration of PAHs within coal tars and found that a modified form of Raoult's law (Eq (3)) is a reasonable estimation of effective concentration. The associated mass balance for the oxidant is given by

$$\frac{dC_{ox}}{dt} = -\frac{(C_{ox} - C_{ox}^{in})}{t_r} - \beta_k k_{ox,k} C_{ox} C_k - \Gamma_{NOI} \quad (6)$$

where C_{ox}^{in} is the inlet oxidant concentration, β_k is the stoichiometric mass ratio defined as the mass of oxidant consumed per mass of constituent degraded, and Γ_{NOI} is the rate of oxidant mass lost to the natural oxidant interaction sink reactions. Details of a representative Γ_{NOI} expression for permanganate are provided by Xu and Thomson (2009), and for persulfate by Sra et al. (2010).

Eqs. (1) and (6) are coupled and must be solved in association with Eqs. (2) to (4) numerically. The following attributes are inherent in this screening model: (i) a completely mixed system (i.e., no preferential flow pathways and infinite dispersion); (ii) mineralization of organic compounds; (iii) the generation of by-products (e.g., manganese oxides, carbon dioxide) are ignored; and (iv) there are no diffusion limitations within the NAPL.

3.0 Results and Discussion

3.1 Batch Experiments

The NOI profiles (average of replicates) for the selected un-impacted aquifer materials are presented in Figure SM-3. For the three (3) aquifer materials tested, the maximum observed consumption of permanganate (expressed as NOD) after 30 days of exposure ranged from of 2 to 5 g/kg. The system pH remained stable between 8 and 9. The permanganate NOD manifested in these batch experiments as an initial rapid increase until Day 7 (NOD_7) followed by a minor increase until Day 30 as it asymptotically approached NOD_{max} (Figure SM-3(a)). The variations between the six series of experiments indicated that, consistent with Xu and Thomson (2009), a higher initial permanganate concentration as well as oxidant to solids mass ratio ($M_{ox/s}$) yielded a higher NOD_{max} and a faster permanganate consumption rate.

For all three of the persulfate systems evaluated (Figures SM-3(b-d)), there was very little loss of persulfate mass (< 10%) after the 30 day reaction period except for the aquifer materials from one borehole location (identified as Sample 1) where the maximum change in persulfate concentration was ~7 g/L (17.5 % decrease). The stability of persulfate in the presence of these aquifer materials implies that there is minimal NOI, and hence persulfate should be persistent *in situ*.

The data generated from the aqueous treatability experiments indicated that all of the 17 dissolved phase compounds detected in the impacted groundwater were readily degraded with persulfate or permanganate (except for benzene) to < MDL by Day 10 for the high (30 g/L) oxidant concentration systems (see Figure 2 for benzene, naphthalene and acenaphthene). As expected, the observed reaction rates for the dissolved phase compounds for the low (5 g/L) oxidant concentration systems were slower. While the oxidant concentration was in excess in all the high oxidant concentration systems, oxidant consumption followed the order: iron-activated persulfate > permanganate > persulfate ≅ alkaline-activated persulfate. Except for benzene, the order of reactivity of the remaining 16 quantified organic compounds was: iron-activated persulfate ≅ permanganate > persulfate ≅ alkaline-activated persulfate. Despite the fact that it was never the intention of these aqueous treatability experiments to generate data that could be used to develop kinetic rate coefficients, a comprehensive analysis of the data was undertaken in an attempt to estimate second-order reaction rate coefficients for all 17 compounds. As expected, due to limited temporal data (2-4 data points for some

compounds), the results yielded only sporadic values and thus no rate coefficients are reported.

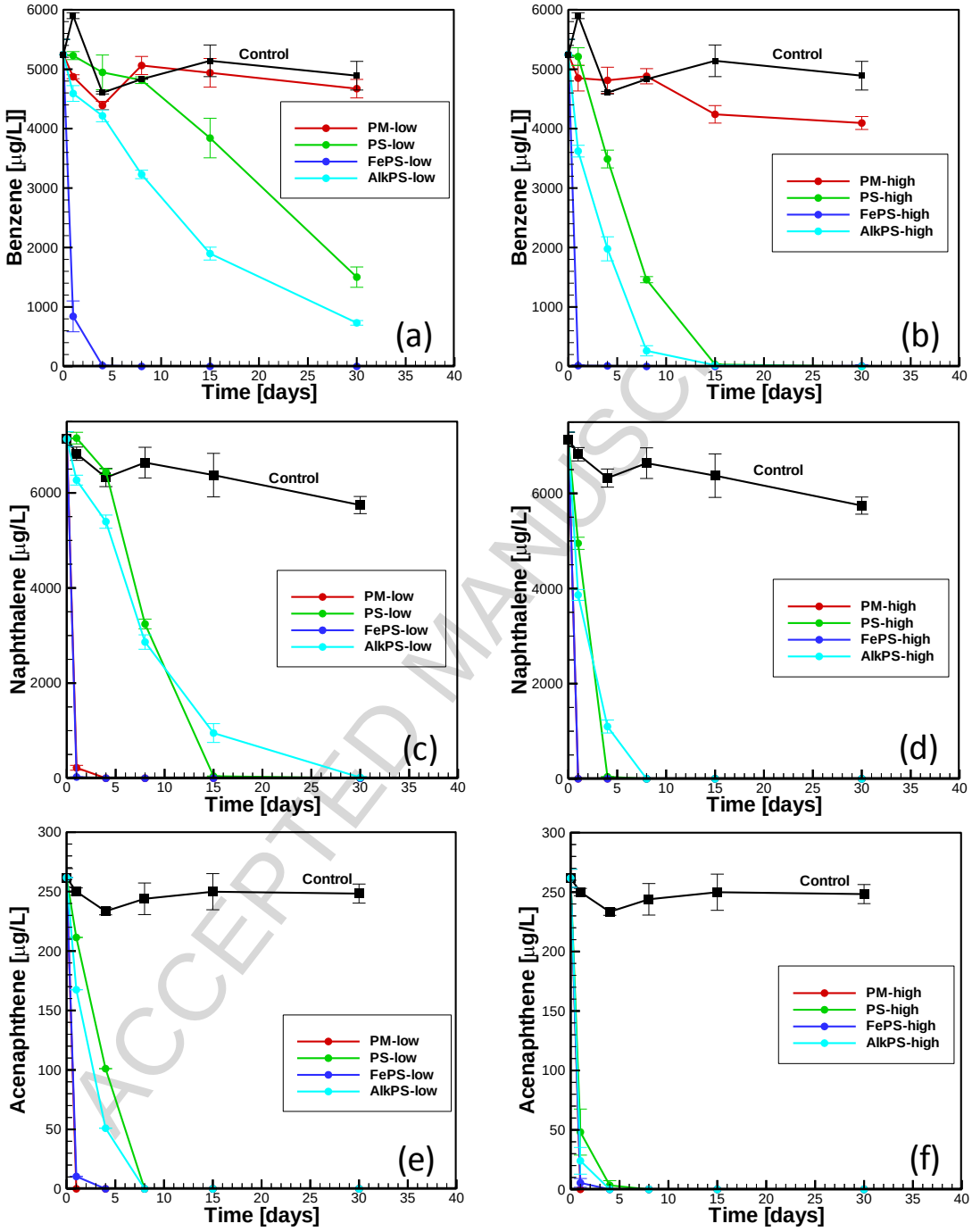

Figure 2. Temporal concentration profiles of (a, b) benzene, (c, d) naphthalene and (e, f) acenaphthene in impacted groundwater exposed to various oxidant systems (permanganate (PM), persulfate (PS), iron activated persulfate (FePS), and alkaline activated persulfate (AlkPS)) at high (30 g/L) and low (5 g/L) concentrations. The error bars represent the standard deviation from triplicate reactors.

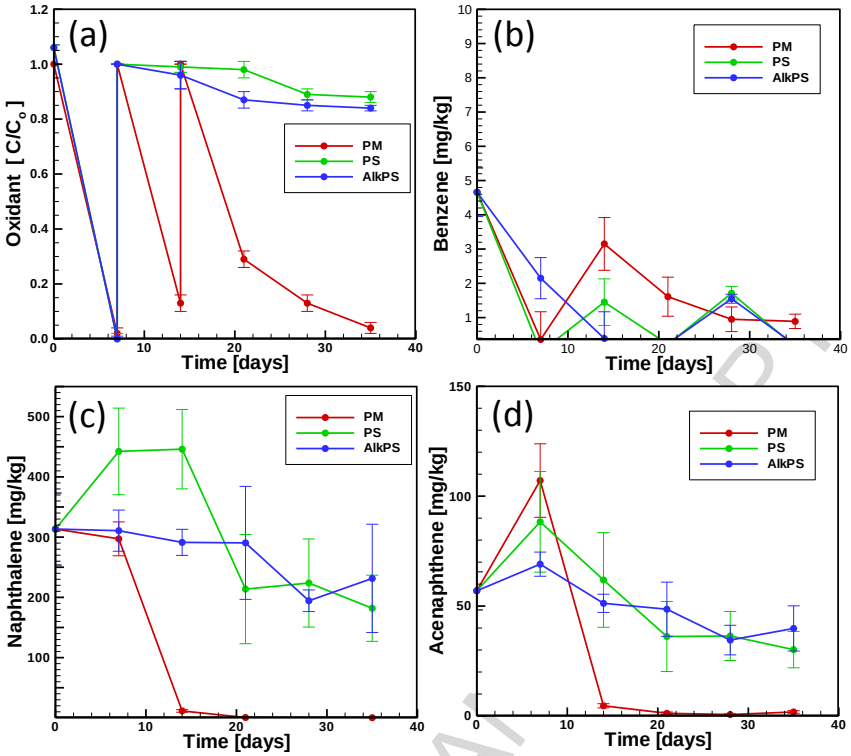

Figure 3. Temporal concentration profiles of (a) oxidant, (b) benzene, (c) naphthalene, and (d) acenaphthene from the slurry experiments. The initial oxidant mass to solids ratio was 30 g/kg for the persulfate (PS), permanganate (PM), and alkaline activated persulfate (AlkPS) systems. The initial oxidant concentration was 30 g/L for all systems. The error bars represent the standard deviation from four replicates.

Temporal oxidant and the bulk soil concentration profiles for naphthalene and acenaphthene from the slurry experimental systems are shown in Figure 3. Although all attempts were made to homogenize the impacted materials prior to adding them to the reactors, there was some variability in the initial bulk soil concentrations of subsamples collected from the "stock" supply of impacted sediments and those emplaced in each reactor. The oxidant mass in the permanganate slurry reactors was replenished at Day 7 and Day 14, while the oxidant mass in the unactivated persulfate and alkaline activated persulfate slurry reactors was replenished only at Day 7. Following replenishment, permanganate continued to be depleted while the concentration of persulfate remained elevated. Compared to either of the persulfate systems explored, permanganate was more effective in treating PAHs (e.g., naphthalene, 1-methylnaphthalene, 2-methylnaphthalene, and acenaphthene) over the 35-day reaction period. For the permanganate, unactivated persulfate, and alkaline activated persulfate

systems it was estimated that 95 %, 45 % and 30 % of the initial mass quantified was degraded, respectively. These values are consistent with the spectrum of mass removal reported by others using batch systems with either permanganate or persulfate (see Table 1). The overall bulk stoichiometry for these slurry experiments was estimated as the ratio of permanganate or persulfate consumed to the quantified mass degraded. These estimates (corrected for NOI) varied from 100 g-$KMnO_4$/g for the permanganate system and 95 g-NaS_2O_8/g for the unactivated persulfate system to 150 g-NaS_2O_8/g for the alkaline activated persulfate system. These stoichiometric values are consistent in magnitude with those reported by Sra et al. (2013) for the total petroleum hydrocarbon (TPH) of dissolved gasoline degraded by various persulfate systems. This data set provides insight into the ability of the investigated oxidant systems to destroy mass present in impacted aquifer materials under ideal conditions (i.e., well mixed, excess oxidant, long contact time) and hence are the most optimistic.

3.2 Physical Models

After 1 to 2 PVs of NaBr injection, the effluent concentration of bromide reached ~50 % of the injected concentration (100 mg/L), and after 3 to 4 PVs reached 100 % for all physical models. Based on the tracer breakthrough profiles the effective porosity for CO-bleb and CO-lense was 0.26 and 0.38 respectively, and ranged from 0.27 to 0.38 for the treatment bleb physical models, and from 0.33 to 0.36 for the treatment lense physical models.

For the control systems (CO-bleb and CO-lense) the effluent pH was steady between 7.5 and 8, and the EC was minimal (< 300 µS/cm) as expected. The concentrations of the detectable organic compounds in the effluent from both control systems were relatively constant except for a notable decrease in the concentration of benzene. The final bulk soil concentrations were essentially unchanged from the initial soil concentrations except for benzene. Benzene was quickly depleted from the system as a result of a higher solubility and lower initial soil concentration compared to other compounds.

For both permanganate systems (PM-bleb and PM-lense) the average naphthalene and acenaphthene effluent concentrations following each oxidant injection episode (~2 PVs/episode) decreased (Figure 4(a, b); see Figure SM-4 for benzene). In contrast, the average naphthalene and acenaphthene effluent concentrations following each oxidant injection episode (~2 PVs/episode) for the persulfate systems either remained relatively

constant (PS-bleb) or increased (PS-lense) (Figure 4(c, d)). These trends were generally consistent for the other monitored compounds except for benzene that remained relatively constant following each persulfate injection episode in the PS-bleb and PS-lense systems.

The average maximum permanganate effluent concentration was ~15 g/L during the first injection episode and increased to ~17 g/L during the second and third injection episodes for the PM-bleb physical models, and was ~17 g/L during the first injection episode and ~20 g/L during the second and third injection episodes for the PM-lense systems. The average maximum persulfate effluent concentration for the PS-bleb physical models was ~23 g/L during the first injection episode and increased to ~25 g/L during the second and third injection episodes. For the PS-lense physical models the average maximum persulfate effluent concentration was ~25 g/L for all injection episodes. The significant reduction of the effluent permanganate or persulfate concentration to near the MDL during the injection of ~3 PVs of degassed Milli-Q water (see Figure SM-5) indicated that remnant oxidant was removed from the experimental system prior to collection of the effluent sample for analyses of organic compounds. The effluent EC profiles were consistent with the permanganate or persulfate effluent profiles.

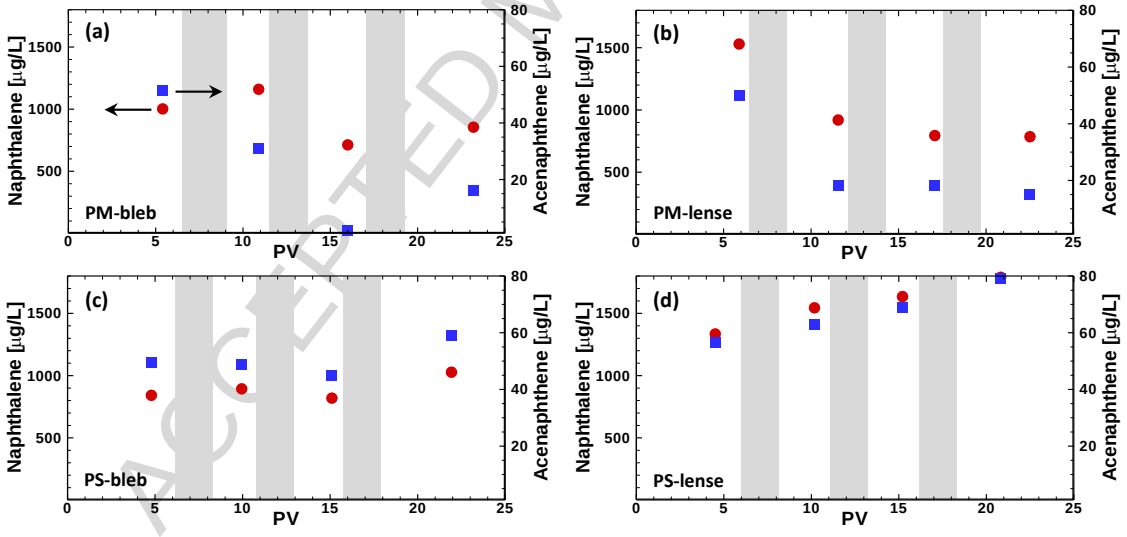

Figure 4. Effluent concentrations for naphthalene (●; left axis) and acenaphthene (■; right axis) from the (a) PM-bleb, (b) PM-lense, (c) PS-bleb and (d) PS-lense physical model experiments. Each data point represents the average from the duplicate physical models. The shaded bands represent the average PV intervals when permanganate or persulfate was injected into each physical model.

The effluent pH for the PM-bleb physical models increased from 7.3 to 9.5 with minor decreases when permanganate was present in the system. In contrast, the effluent pH for the PM-lense physical models oscillated between 7.6 and 9.4. The effluent pH remained relatively stable at 7.9 for the PS-belb and 7.6 for the PS-lense systems.

An evaluation of the initial and final bulk soil concentration data indicated that there was no statistically significant reduction in the total quantifiable mass for all treatment systems at the 5 % level of significance. It is suspected that any decrease in mass was masked by the inherent variability in the soil sub-sampling procedure used and the contaminant heterogeneity present in the physical models. The minor decreases observed in the effluent concentrations following each oxidant injection episode, at least for the permanganate systems (Figure 4(a,b)), indicate that 6 PVs of oxidant treatment had perhaps a minor impact on mass removal but it was not statistically significant. The insignificant mass removal observed in these physical model systems is consistent with the findings from Richardson et al. (2011) who observed no reduction in PAH mass from column experiments using a heat-activated persulfate system (see Table 1). In contrast, Hauswirth and Miller (2014) observed 53% removal in a column experiment after injecting 52 PVs of a 50 g/L alkaline-activated persulfate solution; oxidant dose of 330 g/g-PAH_T compared to the order-of-magnitude smaller oxidant dose of 10 g/g-PAH_T used in this study.

Oxidant mass balance calculations for the bleb systems indicated that 50 and 17 % of the permanganate and persulfate mass injected was consumed, respectively; while for the lense systems 35 and 19 % of the permanganate and persulfate mass injected was consumed, respectively. Hence, while persulfate consumption was similar in the bleb and lense systems, permanganate consumption in the bleb systems was more significant and can be attributed to higher NAPL-aqueous phase contact area. During the 3 oxidant injection episodes (6 PVs total), elevated oxidant concentrations (> 5 g/L) were present for a total residence or contact time of ~8 days. The oxidant resident time was controlled by the flow rate, which was established to yield a moderate linear velocity of 10 cm/day. It was not the objective of these physical model experiments to degrade all the quantified mass present but rather to determine treatment expectations under realistic aggressive conditions. If the intent were to degrade all the mass present then ~33.8 g of oxidant would have been required to degrade 100 % of the initial quantified mass in either the bleb or lenses system. This oxidant demand estimate is based on a stoichiometry ~100 g-oxidant/g of the initial quantified mass estimated from the slurry

experiments. The bulk soil concentration of the aquifer material used in the lense system was about 100 % larger than that using in the bleb system but only half of the physical model was filled with impacted material. Each physical model received a total of ~3.8 g of oxidant, or about 10 % of the stoichiometric requirement delivered in 6 PVs. A typical injection event at the field-scale is less than 1 PV (Huling et al, 2017; Crimi et al., 2011) so it would be a significant effort involving multiple mobilizations over several months to deliver the stoichiometric requirement. Since the oxidant mass that can be delivered per injection event is limited in practice, multiple mobilization events are required and tempered by economic considerations.

Overall, the data from these experiments indicate that the behavior of the physical models with the lense architecture was comparable to those with the bleb architecture. This similarity is likely a direct result of insufficient NAPL concentration in the aquifer materials used to pack the bottom half of the lense physical models. Permanganate outperformed persulfate in terms of affecting a change to the system effluent concentration; albeit this change was minor (there was an insignificant change for persulfate). Despite the observation of better efficiency in the permanganate systems, the total mass removal was low for both systems and hence the benefit of flushing 6 PVs of permanganate or persulfate at a concentration of 30 g/L under the physical model operating conditions was minimal.

3.3 Screening Model Simulations

3.3.1 Parametrization

Consistent with the physical model dimensions, the system length and cross-sectional area were set equal to 7.7 cm and 8.37 cm^2 respectively. This screening model was able to capture the hydraulic and solute transport behaviour observed in the small-scale physical model systems (e.g., see Figure SM-6). The effective porosity values estimated were: 0.28 for PM-bleb, and 0.35 for PM-lense, PS-bleb, and PS-lense. These porosity values are close to the assumed value of 0.3 that was used for the initial nominal PV calculation. The system velocity was assigned a value of 10 cm/day, which is consistent with the average flow rate, cross-sectional area and effective porosity used for the physical model systems.

To reduce model complexity, 22 representative organic compounds (Table 2) were extracted from the NAPL analytical results (Table SM-1) and used to represent the initial NAPL composition. These 22 compounds represent 29% of the NAPL mass, and the

remaining bulk NAPL mass include some identified compounds (~5 %) and the unidentified fraction (~66 %). NAPL saturation for each physical model system was estimated from the initial bulk soil concentration data, bulk density and NAPL composition. The average NAPL saturation values estimated were: 6.4% for PM-bleb, 6.6% for PM-lense, 4.3% for PS-bleb, and 7.9% for PS-lense. Representative NAPL constituent solubility and fugacity data were obtained from the literature (Lide 1999; Eberhardt & Grathwohl 2002; Thomson et al. 2008; Peters et al. 1997).

Since higher treatment efficiency was observed in the physical model systems using permanganate, we choose to focus exclusively on permanganate in these screening model simulations. Literature values (Forsey et al., 2010; Forsey, 2004; Thomson et al., 2008) for the second-order oxidant reaction rate coefficients for permanganate were used for most of the 22 representative organic compounds (Table 2). Missing values for the second-order oxidant rate coefficient were assumed based on structure and trends observed from the aqueous batch experiments. Theoretical values were used for the permanganate/organic compound stoichiometry mass ratio (β) (Table 2).

To capture the consumption of permanganate by the aquifer material, the NOD kinetic model developed by Xu and Thomson (2009) was fit to the data from Series 3 for Sample 1 aquifer material (see left panel in Figure SM-3(a)). In this kinetic model, the rate of change of permanganate is expressed by

$$\frac{d\,(\theta\, C_{ox}\, V_T)}{dt} = -k_{ox}^{fast}\,\theta\, C_{OAM}^{fast}\; C_{ox}\, V_T \;-\; k_{ox}^{slow}\,\theta\, C_{OAM}^{slow}\; C_{ox}\, V_T \tag{7}$$

and the rate of change of the fast and slow reacting oxidizable aquifer material (OAM) species is given by

$$\frac{d\; C_{OAM}^{fast}\; V_T}{dt} = -k_{OAM}^{fast}\;\; C_{OAM}^{fast}\;\; C_{ox}\, V_T \tag{8}$$

and

$$\frac{d\; C_{OAM}^{slow}\; V_T}{dt} = -k_{OAM}^{slow}\;\; C_{OAM}^{slow}\;\; C_{ox}\, V_T \tag{9}$$

where C_{ox} is the aqueous concentration of permanganate expressed as mass of MnO_4^- per volume of solution, C_{OAM}^{fast} and C_{OAM}^{slow} is the concentration of the fast and slow fraction of the bulk OAM expressed as mass of OAM per volume of the system; k_{ox}^{fast} and k_{ox}^{slow}

are the fast and slow reaction rate coefficients with respect to permanganate, k_{OAM}^{fast} and k_{OAM}^{slow} are the fast and slow reaction rate coefficients with respect to OAM, θ is the porosity of the system (solution volume / system volume), and V_T is the total system volume. Based on mass balance considerations the permanganate mass required per unit mass of OAM (g of MnO_4^-/g of OAM) or stoichiometric mass ratio can be expressed as

$$\beta^{fast} = \frac{k_{ox}^{fast}\,\theta}{k_{OAM}^{fast}}, \quad \text{and} \quad \beta^{slow} = \frac{k_{ox}^{slow}\,\theta}{k_{OAM}^{slow}} \tag{10}$$

The calibration results for this kinetic model are shown on Figure SM-7 along with the model parameters. Eqs (7) was implemented into the screening model as the NOI sink term in Eq (6), and Eqs (8-10) were used to represent the mass balance of the fast and slow reacting OAM.

The lumped mass transfer rate coefficient (λ_k) captures the complex dissolution process within the system reflecting, among other factors, the NAPL architecture. β_o in Eq (4) was determined through a calibration procedure that involved the minimization of the weighted sum-of-squares of the difference between the observed (C_i^{obs}) and simulated (C_i^{sim}) baseline concentrations as given by

$$RSS = \sum_{i=1}^{n} \left[\frac{(C_i^{obs} - C_i^{sim})^2}{C_i^{obs}} \right] \tag{11}$$

where n is the number of observations. The observations from first sampling episode (Step 3) for the two PM-bleb systems, and for the two PM-lense systems were separately pooled (n = 16) and used to determine a representative β_o for each system. The calibrated β_o value for the PM-bleb system was 0.61 and resulted in an average λ_k of 0.08/day (min of 0.072/day, max of 0.088/day), and the calibrated β_o value for the PM-lense system was 1.1 and resulted in an average λ_k of 0.14/day (min of 0.131 /day, max of 0.160/day). The slightly higher average λ_k value for the lense system is presumably due to the higher NAPL saturation that results in more NAPL-water contact area and a higher dissolution rate. The scatter plot for the PM-bleb system (Figure SM-8) shows that the model under-predicted the concentration xylene. This is likely caused by slight differences in the NAPL composition assigned to the model and the composition of the impacted aquifer materials used in the physical models.

The observed tracer test behaviour in conjunction with the initial NAPL saturation estimates and the lumped mass transfer coefficient values indicate that, despite all attempts to create two distinct NAPL architectures, both the bleb and lense systems were very similar. This is consistent with the experimental observations.

3.3.2 Benchmarking

The parametrized model was used to simulate the two permanganate physical model systems (PM-bleb, and PM-lense). Not surprising, the overall simulated mass of permanganate consumed was less than that observed. Within this screening model, permanganate consumption results from the oxidation reactions with organic compounds Eq (6) and the NOD Eq (7). The stoichiometric mass ratios (mass of oxidant consumed per mass of organic compound degraded) listed in Table 2 are defined by representative mineralization reactions and are subject to uncertainty since the degradation pathways are not fully understood. In addition, there are likely dissolved compounds present in the system beyond those listed in Table 2. To account for this additional permanganate mass consumed, we assumed that a combination of incorrect stoichiometry and the presence of other dissolved compounds were responsible for the increased observed permanganate consumption. As an alternative to adding an additional permanganate mass sink into the screening model, we elected to multiple the stoichiometric mass ratios by a uniform and constant value. This approach is reasonable since it both increases the stoichiometric mass ratio of those compounds directly simulated, and accounts for a variety of other dissolved compounds that are not simulated in the model but may have similar dissolution behaviour as those simulated. This multiplication factor was estimated by minimizing the sum-of-squares between the simulated effluent concentration profiles for the three injection episodes and the average observed effluent concentration profiles (see upper left panel in Figures 5 and 6). For example, the stoichiometric mass ratio multiplication factor was 140 for the PM-bleb system and resulted in ~1.0 g of additional permanganate being consumed.

Figures 5 and 6 show the simulated effluent concentrations for three representative organic compounds (benzene, naphthalene, and acenaphthene) for the PM-bleb and PM-lense systems respectively along with the observed concentrations from the physical model systems. The concentration of all the organic compounds initially increase from zero (initial condition) until the first permanganate injection episode occurs at 6 PVs. When permanganate is present in the system all the reactive compounds are degraded

to < MDL. This behavior is consistent with observations from a series of preliminary experiments (for example, see data in Table SM-5), and by extension was presumed to be to the case in the experimental data shown on Figures 5 and 6 since the observed permanganate effluent concentrations are elevated. Once the injection solution was switched from permanganate to Milli-Q water, and the permanganate mass was depleted from the system there was a marked rebound in the effluent concentrations. Benzene is not reactive with permanganate and hence follows a steady dissolution profile. The simulation results from the PM-bleb system indicate that during 25 PVs of combined oxidant and water flushing conditions ~0.74 mg or 0.2 % of the initial quantified mass was removed, and 1.3 g of permanganate was consumed.

Since average parameter values were used for the simulations, there is a minor mismatch in timing between the simulated and observed effluent observations. The slight variation (less than an order-of-magnitude) between the simulated and observed rebound concentrations is a result of the heterogeneous nature of the MGP residuals loaded into each physical model, and the assumed initial composition of MGP NAPL used in the simulations (Table 2). No attempt was made to alter the initial NAPL composition to improve the match between the simulated and observed rebound concentrations. Again, based on a series of preliminary experiments it was presumed that when permanganate was present in the system the concentration of organic compounds of interest were <MDL; however, we did not add this assumed behavior to the data shown on Figures 5 and 6. Despite these characteristics, this screening-level model was able to simulate the general observed concentration trends of 23 dissolved organic components as well as the concentration of permanganate for 25 PVs. The performance of this simple screening-level model constrained by the collective dataset was considered to be sufficient evidence for this model to be used to (1) investigate potential conditions required to achieve significant mass removal and (2) understand the long-term behavior of dissolved phase concertation following treatment.

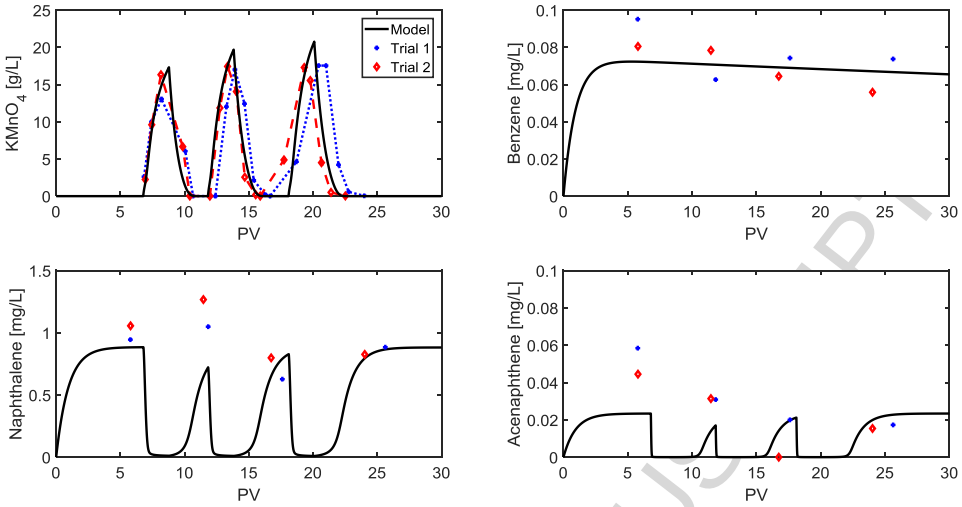

Figure 5. Simulated effluent concentrations for permanganate and three representative organic compounds (benzene, naphthalene, and acenaphthene) for the PM-bleb system. Also shown are observed effluent concentrations.

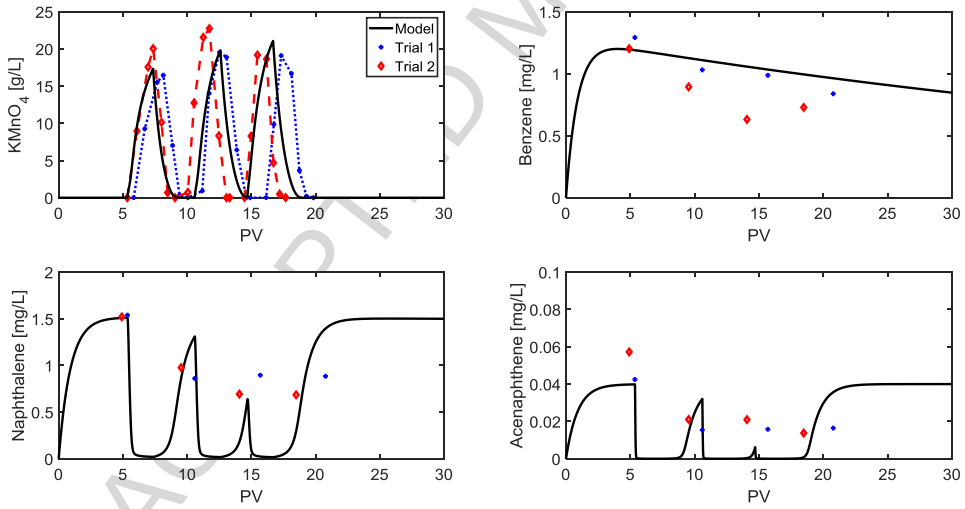

Figure 6. Simulated effluent concentrations for permanganate and three representative organic compounds (benzene, naphthalene, and acenaphthene) for PM-lense system. Also shown are observed effluent concentrations.

3.3.3 Oxidation of Quantified Mass

The results from the physical model experiments and screening model revealed that while >50 % of injected permanganate mass was not consumed, the total mass removed (dissolved and oxidized) during 25 PVs of flushing was minimal. In contrast, the results

from the slurry experiments indicated that under well-mixed conditions with sufficient mass of oxidant present ~95 % the quantified mass was degraded (Figure 3). Hence, it is of interest to explore potential conditions that are required to achieve significant mass removal from the physical model system by oxidation when the stoichiometric mass of oxidant is delivered.

For this hypothetical investigation, we ignored NOD and the stoichiometric mass ratio multiplication factor, and estimated the mass of permanganate required to degrade the total FMGP mass present in the system from

$$M^{T}_{PM} = \sum_{i=1}^{n} \beta_i C_i^n \rho_n S_n \theta V_T \qquad (12)$$

where M^{T}_{PM} is the total mass of $KMnO_4$ required to completely degrade the quantified mass, C_i^n is NAPL concentration of each organic compound, and ρ_n is bulk NAPL density (1.04 g/cm^3). Using the parameters for a representative PM-bleb system in conjunction with data from Table 2, the required mass of permanganate to satisfy the stoichiometric requirement is 6.4 g-$KMnO_4$. For simulation purposes, we assumed that this mass of permanganate was delivered continuous in 25 PVs (injection concentration of 14.2 g-$KMnO_4$/L). As noted previously, at an actual field site the delivery of 3 PVs of an oxidant solution would be considerate aggressive; however, we used 25 PVs here to be consistent with the total number of PVs flushed though the physical models (e.g., see Figure 5). The influence of variations in flow rate and mass transfer rate coefficient on the mass removed by oxidation was explored. The flow rate affects the hydraulic residence time (HRT) or contact time, while the mass transfer rate coefficient controls the availability of dissolved phase organic compounds. Since the mass transfer rate coefficient (Eq. (4)) depends on the organic compound and velocity (and hence flow rate), we multiplied λ_k by a scaling factor ("λ scaling factor") to capture first-order variations in this important process.

The results of this numerical investigation are presented in Figure 7 as the fraction of mass oxidized by permanganate to the initial mass quantified in the system in response to a range of HRT and λ scaling factor values. The white arrow on Figure 7 indicates the conditions (average λ_k of 0.08 /day, and HRT of 0.77 days) representative of the PM-bleb physical model experiments where ~0.2 % of the quantified mass was oxidized. If λ_k is increased by 10^4 for the same HRT of 0.77 days, ~ 60% of the initial mass is oxidized. However, to achieve a higher mass oxidized within the system, the HRT needs

to be increased (flow rate reduced) so that more oxidant remains in the system and is available for oxidation reactions. For example, if the HRT is increased to 35 days, ~90% of the mass is oxidized for a λ scaling factor of 10^4. To achieve > 95% mass oxidized for a λ scaling factor of 10^4, the HRT would need to be > 10^5 days (> 250 yrs) which is clearly unrealistic and essentially mimics a batch reactor. A lumped mass transfer rate coefficient for naphthalene of ~4000/day was reported by Ghoshal et al. (1996) for a flow-through system using coal tar coated silica beads. This value is 5x10^4 larger than the average λ_k (0.08 /day) determined from our physical model experiments, suggesting that the larger λ values in Figure 7 are possible under specific conditions. We acknowledge that in an actual field setting, oxidant mass that is not utilized within the treatment zone would be available to degrade downgradient mass (if present); however, this is not considered here. In addition, this system behavior is subject to the idealized nature of this simple screening level model and associated assumptions.

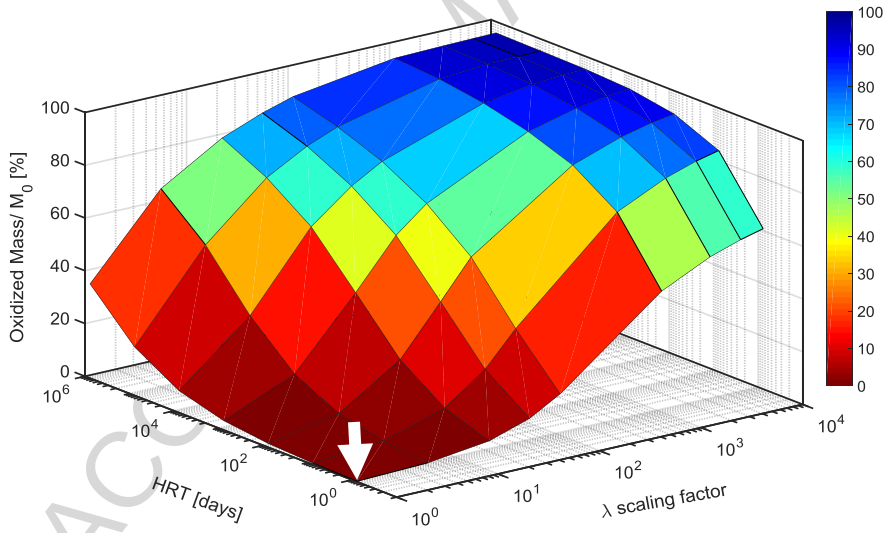

Figure 7. Ratio of mass oxidized by permanganate to the initial mass (M_0) in the system after flushing with 14.2 g-$KMnO_4$/L solution for 25 PVs in response to changes in the hydraulic residence time (HRT) and λ scaling factor as estimated by the screening model. The λ scaling factor was used to multiple the mass transfer rate coefficient (Eq. (4)). The mass of permanganate delivered was sufficient to satisfy the stoichiometric requirement as defined in Table 2. The white arrow indicates the conditions (average λ_k

of 0.08 /day, and HRT of 0.77 days) representative of the PM-bleb physical model experiments.

3.3.4 Long-Term Impacts on Dissolved Phase Concentrations

An understanding of the expected long-term behaviour of dissolved phase concentrations following treatment is crucial to establish the benefit of a remedial effort and for risk assessment. The analysis presented in the previous section focussed on the mass removed within the system as a result of reactions with permanganate. In contrast, we now are interested in the temporal dissolved phase concentrations profiles in the effluent from the treatment system. To determine these concentration profiles, the constrained screening model for the PM-bleb system was used to simulate behaviour over a 5-year period. Permanganate consumption from NOD reactions and the stoichiometric mass ratio multiplication factor were included. The effects of a lower pore velocity (0.1 cm/day compared to 10 cm/day) and higher mass transfer rate coefficient (100 times increase of the average λ_k) on the following three scenarios were separately investigated:

i. *No-Treatment Scenario* – no permanganate injection
ii. *6-PV Oxidant Injection Scenario* - 6 PVs of permanganate (30 g/L) injected in 3 episodes (identical to the oxidant dosing pattern used in the physical model experiments).
iii. *One-year Oxidant Injection Scenario* – continuous permanganate injection for 1 year at 30 or 300 g/L.

Figure 8 shows the dissolved phase concentrations profiles over the 5-yr simulation period for three representative organic compounds (benzene, naphthalene, and acenaphthene) for all three scenarios. Naphthalene is the most abundant and soluble PAH compound present in the system; acenaphthene is soluble, abundant and highly reactive with permanganate relative to naphthalene; and benzene is also soluble and abundant but is not reactive with permanganate. For the base condition velocity of 10 cm/day used, a total of 2400 PVs are flushed through the treatment zone over the 5-year period. As expected, except for benzene that does not react with permanganate, the concentration of the organic compounds are reduced temporality as a result of the presence of permanganate and then rebound to a profile that is essentially coincident with a No-treatment Scenario for both the 6-PV Oxidant Injection and One-year Oxidant Injection Scenarios. Table 3 provides a summary of the mass removed and oxidant consumption for all scenarios. For the 6-PV Oxidant Injection Scenario, ~0.1 % of the quantified mass was degraded by permanganate and > 50 % of the injected

permanganate mass was not consumed. In contrast, for one-year of continuous oxidant injection the quantified mass oxidized increased to ~4 % but the total mass removed did not change significantly (16.7 % compared to 16.5 %), and just 14.4 % of the injected permanganate mass was consumed. These results indicate that injecting a 30 g-$KMnO_4$/L solution for 6 PVs or one year (equivalent to 475 PVs), both considered aggressive approaches, will not materially affect the long-term behavior of dissolved phase concentrations relative to the *No-Treatment Scenario*.

As illustrated on Figure 7, the pore velocity directly affects the contact or residence time, and higher HRT values result in an increase in the mass oxidized within the system. To evaluate how a larger HRT affects dissolved phase concentrations profiles, the pore velocity was decreased by two orders-of-magnitude (from 10 cm/day to 0.1 cm/day). As a direct result of the lower velocity, the total PVs flushed through the treatment system over 5 years is 100 times less (24 vs 2400 PVs). With this larger HRT value, most of the

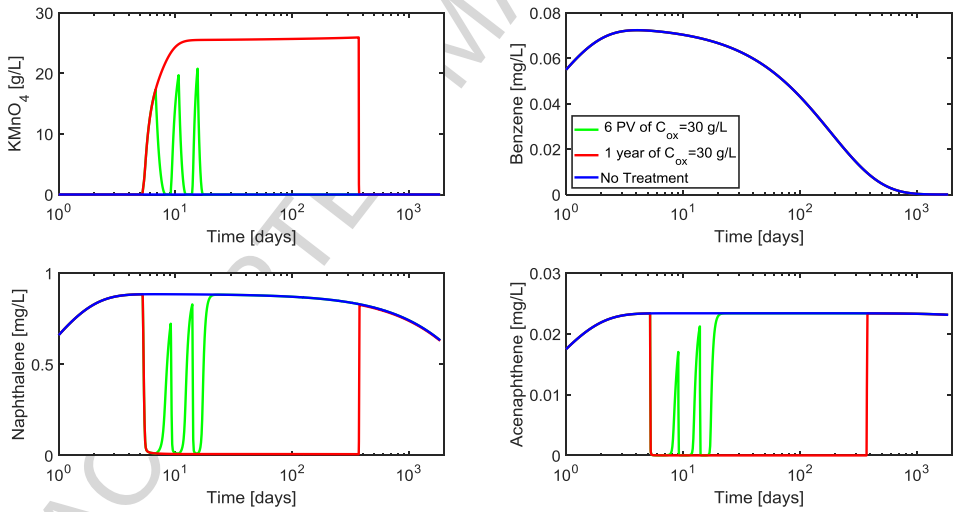

Figure 8. Simulated effluent concentrations from the treatment zone for permanganate, and three representative organic compounds (benzene, naphthalene, and acenaphthene) for the three scenarios investigated over a 5-year period. An average λ_k of 0.08 /day, and velocity of 10 cm/day were used.

permanganate mass injected is consumed (Figure 9 and Table 3). The effluent permanganate concentration reached a maximum of ~0.07 and 0.1 g/L for the 6-PV Oxidant Injection and One-year Oxidant Injection Scenarios, respectively. The effluent organic compound concentrations with the slower velocity (higher HRT) are ~5 times higher than those generated for a velocity of 10 cm/day. The total mass removed and mass oxidized are identical for both the 6-PV Oxidant Injection and One-year Oxidant Injection Scenarios (Table 3). For the lower velocity, only 4.75 PVs of permanganate are injected into the system in 1 year, which is close to 6 PVs so the consistency between the results from these two scenarios is expected. Overall, the total mass removed is significantly lower compared to the mass removed for a velocity of 10 cm/day (1.1 vs 16.6 %) since the mass transfer rate coefficients for the lower velocity of 0.1 /day are ~16 times smaller (average λ_k of 0.005 /day). To provide the treatment system with additional oxidant mass, the permanganate injection concentration was increased by an order-of-magnitude in the One-year Oxidant Injection Scenario from 30 to 300 g-$KMnO_4$/L; an unrealistic value since the solubility of $KMnO_4$ in water is only 64 g/L at 20 °C (Petri et al., 2011a). The results from this simulation show that only 17% of the injected permanganate mass was consumed and that the higher permanganate dosing was not able to increase mass removal (Table 3) nor affect the dissolved phase concentrations profiles (Figure 9). Despite the two order-of-magnitude increase in system residence time, no material changes in the total mass removed and dissolved phase concentrations profiles compared to the No-Treatment Scenario were observed.

As expected, by increasing the average lumped mass transfer rate coefficient by two orders-of-magnitude, the effluent permanganate concentration decreased and the effluent concentration of organic compounds increased (Figure 10). Increasing the lumped mass transfer rate coefficient increases the dissolution rate thus allowing more mass of organic compounds to be available in the aqueous phase for oxidation. After 5 years, ~71% of the initial mass quantified is removed from the treatment system by oxidation and dissolution for the No-Treatment and 6-PV Oxidant Injection Scenarios (Table 3). While ~28% of the initial mass quantified is removed by oxidation in the One-year Oxidant Injection Scenario, this only results in a slight increase of the total mass removed of ~76% compared to the No-Treatment Scenario. By ~100 days benzene is completely depleted from the system due to its higher solubility, and the dissolved phase

concentration profiles for other organic compounds (e.g., naphthalene, and acenaphthene) rebound to

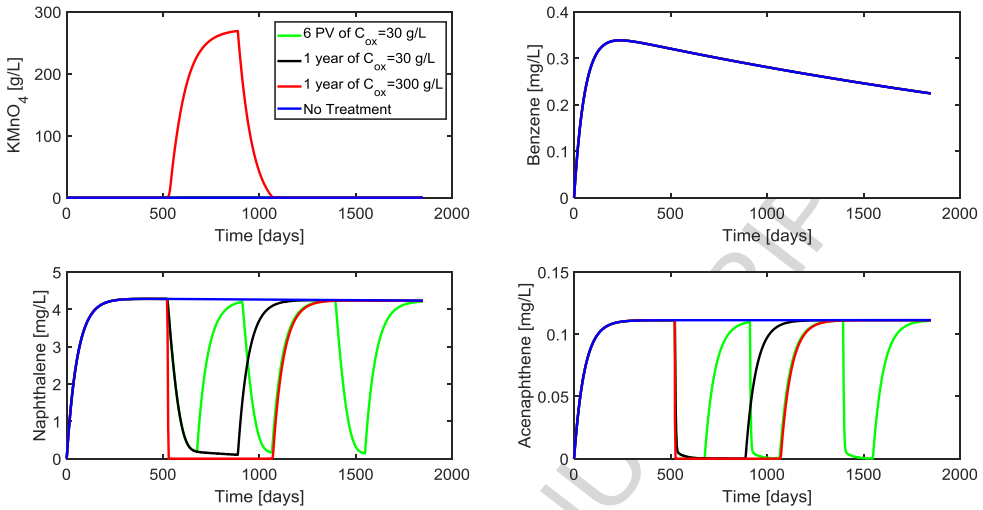

Figure 9. Simulated effluent concentrations from the treatment zone for permanganate, and three representative organic compounds (benzene, naphthalene, and acenaphthene) for the three scenarios investigated over a 5-year period. An average λ_k of 0.08 /day, and velocity of 0.10 cm/day were used.

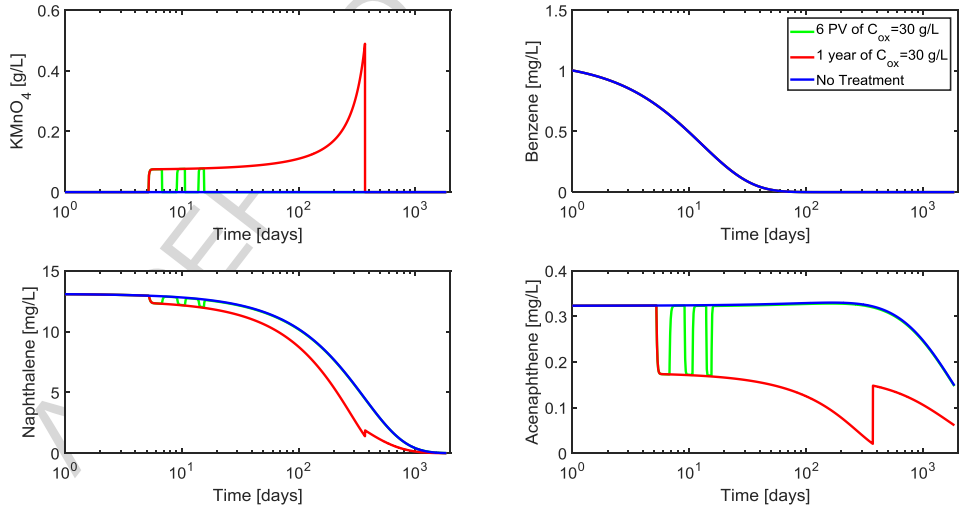

Figure 10. Simulated effluent concentrations from the treatment zone for permanganate, and three representative organic compounds (benzene, naphthalene, and acenaphthene) for the three scenarios investigated over a 5-year period. A velocity of 10 cm/day, and a 100 times increase in the average λ_k of 0.08 /day were used.

concentrations below those for the No-Treatment Scenario once permanganate is no longer present in the system for the One-year Oxidant Injection Scenario only (Figure 10).

In summary, these results indicate that scenarios that involved a lower velocity (0.1 cm/day compared to 10 cm/day) and a higher oxidant dosing were unable to significantly alter the dissolved phase concentrations profiles. In contrast, an increase in the lumped mass transfer rate coefficients by two orders-of-magnitude did have an effect on the dissolved phase concentrations. These results provide additional evidence that treatment efficiency by permanganate is mass transfer limited in this system.

4.0 Summary

The focus of this research effort was to investigate the performance of persulfate and permanganate to degrade FMGP residuals in a flow system representative of *in situ* conditions, and to explore treatment expectations including the long-term behavior of dissolved phase concentrations. The key findings determined are:

- Approximately 29% of the NAPL mass was quantified (72% unidentified and categorized as bulk NAPL); hence our understanding of the behavior of the bulk NAPL mass is uncertain. However, based on analytical data collected, the bulk NAPL is generally considered to consist of low solubility components and as a result is not readily treated by chemical oxidants.
- The dissolved phase components were readily degraded with persulfate or permanganate (except for benzene) in well-mixed aqueous and slurry batch systems. For example in the slurry systems, 95%, 45% and 30% of the initial mass quantified was degraded by permanganate, unactivated persulfate, and alkaline activated persulfate, respectively. As a result of the well-mixed conditions employed, the batch experiment results provide the most optimistic outcome and can be used to bound the expectations for the effectiveness of chemical oxidation of MGP residuals.
- Physical model experiments were performed to evaluate the effects of 6 PVs of oxidant treatment (3 injection episodes at 2 PVs/episode) by either persulfate or permanganate. This is considered an aggressive ISCO approach. Permanganate outperformed persulfate in terms of affecting a change to the system effluent concentration. Despite this observation, the total mass removed was insignificant for

both systems and hence the benefit of flushing 6 PVs of permanganate or persulfate at a concentration of 30 g/L under the physical model operating conditions was deemed minimal.

- The developed screening model was able to capture the general behavior (trends and concentration magnitude) observed in the small-scale physical model experiments.
- Since insignificant mass was degraded in the physical model experiments compared to the slurry batch reactors, the developed screening model was used to determine the potential conditions required so that all of the quantified mass in the system is degraded when sufficient oxidant is present. The results from this evaluation indicated that for larger λ (scaling factor > 100) and HRT (> 10 days) values compared to those determined for the physical model experiments (λ of 0.08 /day, HRT of 0.77 days), permanganate can degrade > 40 % of the initial quantified mass.
- The screening model was used to estimate dissolved phase concentrations for 5 years following exposure to permanganate. The model input parameters were constrained by literature data and the physical model experimental results. The model projected the following
  - the concentration of the organic compounds are reduced temporality as a result of the presence of permanganate and then rebound to a profile that is essentially coincident with a no-treatment scenario despite the presence of excess mass of permanganate;
  - scenarios that involved a lower velocity (0.1 cm/day compared to 10 cm/day) and higher permanganate dosing were unable to significantly alter the long-term dissolved phase concentration profiles;
  - increasing the lumped mass transfer rate coefficients by two orders-of-magnitude resulted in a decrease in the dissolved phase concentration profiles relative to the No-Treatment Scenario once permanganate left the system for a scenario that involved the continuous injection of oxidant for 1 year;
- The collective evidence strongly suggests that treatment of the FMGP residuals explored in this work using chemical oxidants (especially persulfate and permanganate) is mass transfer limited.

5.0 Acknowledgements

Financial support for this investigation was provided by TECO Peoples Gas, Tampa FL, and a Natural Sciences and Engineering Research Council (NSERC) of Canada Collaborative Research and Development Grant (N.R. Thomson).

6.0 References

APHA (American Public Health Association and America Water Works Association, 1998. Standard Methods for the Examination of Water and Sewage, 20th ed., New York.

Birak, P.S., & Miller, C.T. (2009). Dense non-aqueous phase liquids at former manufactured gas plants: challenges to modeling and remediation. *Journal of Contaminant Hydrology*, *105*(3–4), 81–98.

Brown's Directory of North American Gas Companies, 1964. Harcourt Brace Jovanovich Publications, Duluth, Minnesota.

Brown, D.G., Gupta, L., Kim, T. H., Keith Moo-Young, H., & Coleman, A. J. (2006). Comparative assessment of coal tars obtained from 10 former manufactured gas plant sites in the Eastern United States. *Chemosphere*, *65*(9), 1562–1569.

Brown, G. S., Barton, L. L., & Thomson, B. M. (2003). Permanganate oxidation of sorbed polycyclic aromatic hydrocarbons. *Waste Management*, *23*, 737–740.

Cassidy, D. P., Srivastava, V. J., Dombrowski, F. J., & Lingle, J. W. (2015). Combining In-Situ Chemical Oxidation, Stabilization and Anaerobic Bioremediation in a Single Application to Reduce Contaminant Mass and Leachability in Soil. *Journal of Hazardous Materials*.

Crimi, M., Simpkin, T.J., Palaia, T., Petri, B.G., & Siegrist, R.L. (2011). Systematic approach for site specific engineering of ISCO. In Situ Chemical Oxidation for Groundwater Remediation, Eds. R.L. Siegrist, M. Crimi, T.J Simpkin, Springer, NY, Ch 9, 355-412.

Eberhardt, C., & Grathwohl, P. (2002). Time scales of organic contaminant dissolution from complex source zones: coal tar pools vs. blobs. *Journal of Contaminant Hydrology*, *59*(1–2), 45–66.

Ferrarese, E., Andreottola, G., & Oprea, I. A. (2008). Remediation of PAH-contaminated sediments by chemical oxidation. *Journal of Hazardous Materials*, *152*(1), 128–39.

Forsey, S. P. (2004). *In situ Chemical Oxidation of Creosote / Coal Tar Residuals : Experimental and Numerical Investigation*. University of Waterloo, ON.

Forsey, S. P., Thomson, N. R., & Barker, J. F. (2010). Oxidation kinetics of polycyclic aromatic hydrocarbons by permanganate. *Chemosphere*, *79*(6), 628–36.

Gan, S., Lau, E. V, & Ng, H. K. (2009). Remediation of soils contaminated with polycyclic aromatic hydrocarbons (PAHs). *Journal of Hazardous Materials*, *172*(2–3), 532–49.

Gates-Anderson, B. D. D., Siegrist, R. L., & Cline, S. R. (2001). Comparison of Potassium Permanganate and Hydrogen Peroxide as Chemical Oxidants for Organically Contaminated Soils. *J. Environ. Eng.*, 337–347.

Ghoshal, S., Ramaswami, A., & Luthy, R. G. (1996). Biodegradation of naphthalene from coal tar and heptamethylnonane in mixed batch systems. Environmental Science and Technology, 30(4), 1282–1291.

Hatheway, A. W. (2012). *Remediation of former manufactured gas plants and other coal-tar sites*. CRC Press, Talor & Francis Group.

Hauswirth, S. C., Birak, P. S., Rylander, S. C., & Miller, C. T. (2012). Mobilization of Manufactured Gas Plant Tar with Alkaline Flushing Solutions. *Environ. Sci. Technol.*, *46*, 426–433.

Hauswirth, S. C., & Miller, C. T. (2014). A comparison of physicochemical methods for the remediation of porous medium systems contaminated with tar. *Journal of Contaminant Hydrology*, *167C*, 44–60.

Huang, K., R.A. Couttenye, G.E. Hoag, 2002. Kinetics of heat-assisted persulfate oxidation of methyl tert-butyl ether (MTBE), Chemosphere, 49, 413-420.

Huling, S.G., R.R. Ross, K.M. Prestbo, 2017. In situ chemical oxidation: Permanganate oxidant volume design considerations. Groundwater Monitoring & Remediation, 37(2), 78-86.

Krembs, F. J., Siegrist, R. L., Crimi, M. L., Furrer, R. F., & Petri, B. G. (2010). ISCO for Groundwater Remediation : Analysis of Field Applications and Performance. *Groundwater Monitoring & Remediation*, *30*(4), 42–53.

Lee, L. S., Rao, P. S. C., & Okuda, I. (1992). Equilibrium partitioning of polycyclic aromatic hydrocarbon from coal tars into water. *Environ. Sci. Technol.*, *26*(11), 2110–2115.

Lemaire, J., Laurent, F., Leyval, C., Schwartz, C., Buès, M., & Simonnot, M.-O. (2013). PAH oxidation in aged and spiked soils investigated by column experiments. *Chemosphere*, *91*(3), 406–14.

Liang, C., Huang, C.-F., Mohanty, N., & Kurakalva, R. M. (2008). A rapid spectrophotometric determination of persulfate anion in ISCO. *Chemosphere*, *73*(9), 1540–3.

Lide, D. R. (1999). *CRC handbook of physics and chemistry*.

Luthy, R. G., Dzombak, D. A., Peters, C. A., Roy, S. B., Ramaswami, A., Nakles, D. V., & Nott, B. R. (1994). Remediating Tar-Contaminated Soils at Manufactured Gas Plant Sites: Technological Challenges. *Environ. Sci. Technol.*, *28*(6), 266A–276A.

McGuire, T. M., McDade, J. M., & Newell, C. J. (2006). Performance of DNAPL source depletion technologies at 59 chlorinated solvent-impacted sites. *Ground Water Monitoring and Remediation*, *26*(1), 73–84.

Mueller, J. G., Chapman, P. J., & Pritchard, P. H. (1989). Creosote-contaminated sites. Their potential for bioremediation. *Environmental Science & Technology*, *23*(10), 1197–1201.

Nadim, F., Huang, K.-C., & Dahmani, A. M. (2005). Remediation of Soil and Ground Water Contaminated with PAH using Heat and Fe(II)-EDTA Catalyzed Persulfate Oxidation. *Water, Air, & Soil Pollution: Focus*, *6*(1–2), 227–232.

Peng, L., Wang, L., Hu, X., Wu, P., Wang, X., Huang, C., X. Wang, Deng, D. (2016). Ultrasound assisted, thermally activated persulfate oxidation of coal tar DNAPLs. *Journal of Hazardous Materials*, *318*, 497–506.

Peters, C. A., Mukherji, S., Knightes, C. D., & Weber, W. (1997). Phase Stability of Multicomponent NAPLs Containing PAHs. *Environ. Sci. Technol.*, *31*(9), 2540–2546.

Petri, B.G., Thomson, N.R., & Urynowicz, M.A. (2011a). Fundamentals of ISCO using permanganate, In Situ Chemical Oxidation for Groundwater Remediation, Eds. R.L. Siegrist, M. Crimi, T.J Simpkin, Springer, NY, Ch 3, 89-146.

Petri, B.G., Watts, R.J., Tsitonaki, A., Crimi, M., Thomson, N.R., & Teel, A.L. (2011b). Fundamentals of ISCO using persulfate, In Situ Chemical Oxidation for Groundwater Remediation, Eds. R.L. Siegrist, M. Crimi, T.J Simpkin, Springer, NY, Ch 4, 147-191.

Powers, S. E., Abriola, L. M., Dunkin, J. S., & Weber, W. J. (1994a). Phenomenological models for transient NAPL-water mass-transfer processes. *Journal of Contaminant Hydrology*, *16*, 1–33.

Powers, S. E., Abriola, L. M., & Weber, W. J. (1994b). An experimental investigation of nonaqueous phase liquid dissolution in saturated subsurface systems : Transient mass transfer rates. Water Resources Research, *30*(2), 321–332.

Richardson, S. D., Lebron, B. L., Miller, C. T., & Aitken, M. D. (2011). Recovery of Phenanthrene-Degrading Bacteria after Simulated in Situ Persulfate Oxidation in Contaminated Soil. *Environ. Sci. Technol.*, *45*(2), 719–725.

Rivas, F.J. (2006). Polycyclic aromatic hydrocarbons sorbed on soils: a short review of

chemical oxidation based treatments. *Journal of Hazardous Materials*, *138*(2), 234–51.

Siegrist, R.L., Crimi, M., Simpkin, T.J., Brown, R.A., & Unger, M. (2011). ISCO status and future directions. In Situ Chemical Oxidation for Groundwater Remediation, Eds. R.L. Siegrist, M. Crimi, T.J Simpkin, Springer, NY, Ch 14, 535-545.

Soga, K., Page, J. W. E., & Illangasekare, T. H. (2004). A review of NAPL source zone remediation efficiency and the mass flux approach. *Journal of Hazardous Materials*, *110*(1–3), 13–27.

Sra, K.S., Thomson, N. R., Barker, J.F. (2013). Persulfate Treatment of Dissolved Gasoline Compounds. *J. Hazardous, Toxic, and Radioactive Waste*, *17*, 9–15..

Sra, K. S., Thomson, N. R., & Barker, J. F. (2010). Persistence of Persulfate in Uncontaminated Aquifer Materials. *Environ. Sci. Technol.*, *44*(8), 3098–3104.

Thomson, N. R., Fraser, M. J., Lamarche, C., Barker, J. F., & Forsey, S. P. (2008). Rebound of a coal tar creosote plume following partial source zone treatment with permanganate. *Journal of Contaminant Hydrology*, *102*(1–2), 154–71.

USEPA, (1999). A Resource for MGP Site Characterization and Remediation, available at https://clu-in.org/download/misc/mgp/chap1-4a.pdf, U.S. Environmental Protection Agency Office of Solid Waste and Emergency Response Technology Innovation Office Washington, DC

USEPA, (2006), Huling, S. G., Pivetz, B. E. Engineering Issue: In-Situ Chemical Oxidation. EPA/600/R- 06/072.U.S.Environmental Protection Agency, Office of Research and Development, National Risk Management Research Laboratory, Cincinnati, OH.

USEPA, (2013). *Superfund Remedy Selection Report, 14th Edition*.EPA 542-R-13-016, Solid Waste and Emergency Response.

Usman, M., Faure, P., Ruby, C., & Hanna, K. (2012). Application of magnetite-activated persulfate oxidation for the degradation of PAHs in contaminated soils. *Chemosphere*, *87*(3), 234–40.

Wang, W., Liu, G., Shen, J., Chang, H., Li, R., Du, J., Yang, Z., Xu, Q. (2015). Reducing polycyclic aromatic hydrocarbons content in coal tar pitch by potassium permanganate oxidation and solvent extraction. *Journal of Environmental Chemical Engineering*.

Xu, X., & Thomson, N. R. (2009). A long-term bench-scale investigation of permanganate consumption by aquifer materials. Journal of Contaminant Hydrology, 110(3–4), 73–86.

Table 1. Summary of published bench-scale studies which have used either persulfate or permanganate to degrade FMGP residuals.

Source	Experimental System	Reaction time or PVs	Material	Organic Concentration	Oxidant System(s)	Oxidant Dose	Removal in soil [%]
This study	batch[1], physical model	batch: 5 weeks, physcial model: 6 PVs	FMGP impacted aquifer material	BTEX = 0.02 & PAH_T = 3.54 g/kg soil (23 compounds)[10]	30 g/L permanganate, 30 g/L persulfate and 30 g/L alkaline activated persulfate	batch:~8.5 g oxidant/g PAH, physical model:~10 g oxidant/g PAH	permanganate batch:~95% of PAH_T, persulfate batch:~45% of PAH_T, physical model: no significant PAH removal in all systems
Peng et al. (2016)	batch[2]	120 min	spiked soil	PAH_T[11] = 6.87 g/kg (20 compounds)	50 g/L ultrasound-heat-activated persulfate (80 °C)	~29 g oxidant/g PAH	~85% of PAH_T
Cassidy et al. (2015)	batch[3]	1 week	FMGP impacted soil	BTEX = 0.58 & PAH_T = 3.06 g/kg soil (18 compounds)	36.6 g/L alkaline activated persulfate	~5 g oxidant/g PAH	55% of BTEX & 64% of PAH_T
Wang et al. (2015)	batch[4]	3 hr	coal tar pitch	PAH_T = 76.50 g/kg (7 compounds)	31.6 g/L permanganate	~2 g oxidant/g PAH	62.5% of carcinogenicity removed
Hauswirth et al. (2014)	column	52 PVs	FMGP impacted soil	PAH_T[12] = 1.99 g/kg (25 compounds)	50 g/L persulfate & 0.2 M NaOH	~330 g oxidant/g PAH	53% of PAH_T
Usman et al. (2012)	batch[5]	1 week	FMGP impacted soil	PAH_T = 1.3 g/kg soil (16 compounds)	iron-activated persulfate (molar ratio 1:1)	not reported	no PAH removal
Richardson et al. (2011)	batch[6], column	batch: 16 days, column: 6 PVs	FMGP impacted soil	PAH_T = 0.295 g/kg soil (14 compounds)	20 g/L heat-activated persulfate (40 °C)	~91 g oxidant/g PAH	batch: 47% of PAH_T, column: no significant PAH removal
Ferrarese et al. (2008)	batch[7]	until consumption of oxidant	canal sediment	PAH_T = 2.8 g/kg soil (16 compounds)	158 g/L permanganate, and 120 g/L Fe activated persulfate (Fe:oxidant molar ratio of 1:25)	188 g permanganate/g PAH; 142 g persulfate/g PAH	permanganate: 96% of PAH_T, persulfate: 88% of PAH_T
Nadim et al. (2005)	batch[8]	24 hr	FMGP impacted soil	PAH_T = 0.01 g/kg soil (7 compounds)	5 g/L persulfate + 0.124 g/L Fe-EDTA	~1500 g oxidant/g PAH	75 to 100% of PAH_T
Brown et al. (2003)	batch[9]	30 min	spiked soil	PAH_T = 0.73 g/kg soil (6 compounds)	25 g/L permanganate	~68.5 g oxidant/g PAH	8 to 72% of PAH_T

Notes:
1. 125 mL reactors filled with 75 g of impacted material and 75 mL oxidant solution, mixed and left in the dark.
2. 5 g surficial soil with 100 mg of laboratory grade coal tar added to a 40 mL vial and mixed with 20 mL oxidant solution.
3. 2.5 L reactors filled with 3 kg soil and mixed with a blender.
4. 20 g crushed coal tar pitch and 100 mL oxidant solution placed in 250 mL reactor and mixed on a shaker.
5. 2 g soil in 20 mL oxidant solution.
6. Batch data not reported.
7. 30 g sediment mixed with 100 mL solution, reactors periodically shaken.

8. 250 mL reactor mixed on a shaker
(liquid : soil ratio = 3.33)
9. 250 mL reactor filled with 50 g soil and 100 mL of
oxidant solution; continuously stirred.
10. Number of
quantified PAH
compounds.
11. Estimated from data
provided.
12. Estimated from data provided, and assuming a NAPL density of 1.1 g/mL
and a bulk density of 1.7 g/mL.

Table 2. NAPL composition, molecular weight (MW), solubility, fugacity ratio (f^S/f^L), permanganate second-order reaction rate coefficient (*k*), and permanganate/organic compound stoichiometry (β) for the representative organic compounds using in the model simulations.

Organic Compound	Concentration[1] [mg/kg]	MW [g/mol]	Solubility[2] [mg/L]	f^S/f^L[2] [-]	*k* [L/g/day]	*B*[3] [g/g]
BTEX						
Benzene	2640	78.1	1780	1.00	0[4]	20.2
Ethylbenzene	4480	106.2	161.2	1.00	3.31[4]	20.8
Xylene(s)	2618	106.0	173.5	1.00	0.389[5]	20.8
Toluene	32.3	92.1	534.8	1.00	0.389[5]	20.6
Trimethylbenzenes						
Trimethylbenzene(s)	3750	120.2	57.4	1.00	0.288[5]	21.0
Methylethylbenzene						
Methylethylbenzene(s)	2275	120.2	94	1.00	0.288[5]	21.0
PAHs						
1-Methylnaphthalene	25500	142.2	28.5	1.00	7.34[6]	20.0
2-Methylnaphthalene	46700	142.2	25.4	0.86	10.5[6]	20.0
2,6-Dimethylnaphthalene	11500	156.2	2.0	1.00	14.4[5]	20.2
Acenaphthene	13300	154.2	3.9	0.20	115[6]	19.8
Acenaphthylene	4050	152.2	9.8	0.22	6.05[5]	19.4
Anthracene	6280	178.2	0.05	0.01	288[5]	16.2
Biphenyl	4990	154.2	7.5	1.00	0[4]	0.0
Chrysene	2810	228.2	0.002	0.01	6.78[4]	19.4
Dibenzofuran	1500	168.2	10.0	0.25	0[4]	16.9
Fluoranthene	7930	202.3	0.26	0.21	475[6]	19.2
Indane	11200	118.0	109.1	1.00	14.4[5]	20.5
Indene	1700	116.2	390	1.00	14.4[5]	20.0
Fluorene	7720	166.2	2.0	0.16	230[6]	19.3
Naphthalene	83800	128.2	31.7	0.30	6.05[6]	19.7
Phenanthrene	26400	178.2	1.18	0.28	230[6]	16.5
Pyrene	12900	202.3	0.13	0.11	864[6]	19.2
Bulk	-	280.0[5]	0	1.00[5]	0[5]	0.0

Notes:

1. from Table SM-1
2. from Peters et al. (1997), Lide (1999), Eberhardt & Grathwohl (2002), and Thomson et al. (2008)
3. theoretical permanganate/organic compound stoichiometric mass ratio
4. from Forsey et al. (2010)
5. assumed values
6. from Thomson et al. (2008)

Table 3: Summary of mass removed by oxidation, mass removed by oxidation and dissolution, and mass of permanganate consumed within the treatment zone over the 5-yr simulation period.

Description	M_{OX} / M_0 [1] [%]	M_T / M_0 [2] [%]	PM_{Con} / PM_{Inj} [3] [%]
Base Conditions (v = 10 cm/day; average λ_k = 0.08 /day)			
No-Treatment Scenario (2400 PVs of water)	-	16.5	-
6-PV Oxidant Injection Scenario (2400 PVs of water)	0.1	16.5	41.3
One-year Oxidant Injection Scenario (475 PVs of 30 g-$KMnO_4$/L then 1925 PVs water)	3.8	16.7	14.4
Decrease in Pore Velocity (*v* = 0.1 cm/day)			
No-Treatment Scenario (24 PVs of water)	-	1.0	-
6-PV Oxidant Injection Scenario (6 PVs 30 g-$KMnO_4$/L then 18 PVs water)	0.3	1.1	99.9
One-year Oxidant Injection Scenario			
(4.75 PVs of 30 g-$KMnO_4$/L then 19.25 PVs water)	0.3	1.1	99.9
(4.75 PVs of 300 g-$KMnO_4$/L then 19.25 PVs water)	0.4	1.1	17.1
Increase in average λ_k (100 x)			
No-Treatment Scenario (2400 PVs of water)	-	70.8	-
6-PV Oxidant Injection Scenario (2400 PVs of water)	0.4	70.9	99.7
One-year Oxidant Injection Scenario (475 PVs of 30 g-$KMnO_4$/L then 1925 PVs water)	27.5	75.9	99.3

Notes:

1. Ratio of quantified mass oxidized (M_{OX}) to initial quantified mass (M_o).

2. Ratio of total mass removed from system by oxidation and dissolution (M_T) to initial quantified mass (M_o).
3. Ratio of mass of permanganate consumed (PM_{Con}) to mass injected (PM_{Inj}).

Highlights

- Possible to degrade 30 to 95% of mass in well-mixed slurry systems
- Insignificant mass degraded by persulfate or permanganate under dynamic conditions
- 6 PVs oxidant injection does not change dissolved phase concentration profiles
- Increase in HRT and mass transfer rate coefficient (λ_k) required to oxidize mass
- Increase in λ_k necessary to alter long-term dissolved phase concentrations